# Navigating Spatial Trade-offs in Restoration Planning: A Multi-Objective Optimization Framework Integrating Ecological Feasibility

Matías Moreno-Faguett[1,2,*], Jessica Castillo-Mandujano[3]; José Salgado-Rojas[1], María José Martinez-Harms[4,5,3], Bárbara Larraín-Barrios[5,3,6,1], Micaela Poutay- Broussaingaray[3], Eduardo Fuentes-Lillo[7,3], Pablo Ramírez de Arellano[8], Patricio Pliscoff[9,3], Cecilia Smith-Ramírez[10,3], Olga Barbosa Prieto[11,3], Aníbal Pauchard[7,3], Jordi Garcia-Gonzalo[1], Virgilio Hermoso[12], Eduardo Álvarez-Miranda[13,6,3]

[1]Centre de Ciència i Tecnologia Forestal de Catalunya, Ctra. St. Llorenç de Morunys km 2, Solsona, 25280, Spain

[2]Instituto de Matemáticas de la Universidad de Sevilla, Universidad de Sevilla, Seville, Spain

[3]Instituto de Ecología y Biodiversidad, Victoria 631, Barrio Universitario, Concepción, Chile

[4]Facultad de Ingeniería y Ciencias, Universidad Adolfo Ibáñez, Santiago, Chile

[5]Millennium Institute in Coastal Socio-Ecology, Pontificia Universidad Católica de Chile, Santiago, Chile

[6]Instituto Sistemas Complejos de Ingeniería, Chile

[7]Laboratorio de Invasiones Biológicas, Facultad de Ciencias Forestales, Universidad de Concepción, Concepción, Chile

[8]Bioforest SA, Camino a Coronel s/n, Coronel, Chile

[9]Centro de Estudios Públicos, Santiago, Chile

[10]Departamento de Ciencias Biológicas y Biodiversidad, Universidad de Los Lagos, Osorno, Chile

[11]Centro de Investigación para la Sustentabilidad, Facultad de Ciencias de La Vida, Universidad Andrés Bello, Chile

[12]Departamento de Biología de la Conservación y Cambio Global, Estación Biológica de Doñana - CSIC, Seville, Spain

[13]Department of Industrial Engineering, Faculty of Engineering, Universidad de Talca, Sede Curicó, Chile

**Corresponding author: matiasmorenofaguett@gmail.com*

**Abstract**

Ecosystem restoration requires decision-support tools capable of balancing ecological benefits under limited resources while explicitly accounting for the long-term likelihood of restoration success. Despite its recognized importance, ecological feasibility has rarely been formulated as an optimization objective in spatial planning, typically being treated only as a constraint or biophysical filter. Here, we present a multi-objective optimization

framework for large-scale restoration planning that explicitly incorporates ecological feasibility alongside biodiversity and ecosystem service objectives. The framework is grounded in Systematic Conservation Planning and formulated as a Mixed-Integer Linear Programming model.

We jointly optimize four criteria—extinction risk reduction, carbon storage, water provision, and ecological feasibility—under a fixed restoration area budget and land suitability constraints. Optimization proceeds in two steps: single-objective benchmark solutions are first obtained to define aspiration levels, which are then integrated using Goal Programming to generate balanced compromise solutions and characterize trade-offs. Ecological feasibility is modeled as a socio-ecological property linked to recurrent disturbance regimes, operationalized through spatial proxies of wildfire frequency, anthropogenic pressure, and invasive species richness.

Applied to continental Chile using 812,910 units at 1 km² resolution, incorporating feasibility leads to significant spatial reconfiguration: approximately 16.6% of selected units (under a 30% restoration target aligned with Target 2 of the Kunming–Montreal Global Biodiversity Framework) are replaced relative to solutions that ignore feasibility. This shift preserves total restored area while increasing feasibility performance by 11.1 percentage points, with minimal reductions (below 5%) in the remaining objectives (−4.1 for carbon storage and −2.4 for water provision). Spatial diagnostics based on selection frequency reveal that compromise solutions are anchored in a "backbone" of multipurpose planning units (> 80% of selected units), complemented by specialized units that resolve localized trade-offs. Overall, the proposed framework provides a transparent and transferable approach for integrating ecological feasibility into spatial restoration planning, enabling more robust and policy-relevant decision-making.

*Keywords:* ecological feasibility; restoration planning; multi-objective optimization; trade-off analysis; goal programming; spatial prioritization

## 1. Introduction

Ecosystem degradation is among the leading global drivers of biodiversity loss and climate vulnerability (MEA, 2005; IPBES, 2019). The United Nations has declared the Decade on Ecosystem Restoration (2021–2030), underscoring the urgent need to halt and reverse ecosystem degradation to safeguard biodiversity, enhance ecosystem services, and mitigate climate change impacts (United Nations, 2024; FAO et al., 2024). To address these global challenges, the Kunming–Montreal Global Biodiversity Framework established ambitious 2030 commitments, including the restoration of at least 30% of degraded terrestrial, freshwater, and marine ecosystems (Target 2) (CBD, 2022). Some countries have adopted these targets as national commitments, implying that restoration prioritization must operate at large scales to coordinate actions and distribute budgets efficiently across political jurisdictions (Eckert et al., 2023; Carroll et al., 2024). Achieving these commitments requires decision-support tools capable of integrating ecological, social, and economic objectives under limited financial and institutional resources to support the efficient allocation of restoration actions (Margules & Pressey, 2000; Bottrill et al., 2008; Menz et al., 2013).

The development of decision-support tools must acknowledge that restoration planning is inherently multi-objective (Castillo-Mandujano & Smith-Ramírez, 2022). Here, we adopt a broad definition of restoration as the process of assisting the recovery of degraded, damaged, or transformed ecosystems to restore ecological functionality, integrity, and biodiversity across multiple dimensions of biotic organization. This requires the simultaneous improvement of biodiversity, the enhancement of ecosystem services—such as climate regulation and water provision—and the explicit consideration of ecological feasibility. Here, ecological feasibility refers to the likelihood that restoration actions will succeed over the long term under prevailing ecological disturbances (MEA, 2005; Orsi & Geneletti, 2010; Aronson et al., 2011; IPBES, 2018; FAO et al., 2024). This concept is distinct from implementation feasibility, which is typically defined by economic or logistical constraints. Ecological feasibility depends on a combination of factors, such as wildfire likelihood, anthropogenic pressures (e.g., proximity to populated areas), and invasive species spread, all of which can compromise restoration outcomes (Orsi et al., 2011). Because these disturbance pressures operate along continuous spatial gradients rather than as strict binary boundaries, treating feasibility merely as an exclusion filter (i.e., hard constraints or locked-out) risks excluding areas with high ecological value. Consequently, restoration planning must move beyond single-objective approaches toward frameworks capable of explicitly integrating trade-offs among benefits, costs, and feasibility at large spatial scales, allowing decision-makers to balance the ecological gains against the varying likelihood of long-term success (Giakoumi et al., 2025; Neubert et al., 2025).

Because restoration involves multiple, often conflicting objectives—where advancing one objective may compromise another—multi-objective optimization (MOO) offers a suitable approach to address this complexity by balancing competing ecological dimensions and evaluating trade-offs (Alagador & Cerdeira, 2022; Neubert et al., 2025). Although these dimensions can also be viewed as decision criteria, hereafter we refer to them as objectives because they are explicitly represented in the optimization model. Within the framework of Systematic Conservation Planning (SCP)—originally developed for biodiversity protection (Margules & Pressey, 2000; Margules & Sarkar, 2007; Wiersma & Sleep, 2016) and increasingly applied to ecological restoration (Kukkala & Moilanen, 2013; McIntosh et al., 2017; Sewall et al., 2011)—several decision-support tools have been developed (Giakoumi et al., 2025; Neubert et al., 2025). Widely used tools like *Marxan with Zones* (Abarca et al., 2022; Domisch et al., 2019; Gurney et al., 2015; Hermoso et al., 2023; Iglesias et al., 2022; Watts et al., 2009) and *Zonation* (Di Minin et al., 2017; Harlio et al., 2019; Moilanen et al., 2022; Sala et al., 2021; Schüler & Bustamante, 2022; Srivathsa et al., 2023), rely on heuristic approaches such as simulated annealing and evolutionary algorithms (Bayer et al., 2023; Dai & Ratick, 2014; Hildemann et al., 2023; Kramer et al., 2013; Schlottfeldt et al., 2015; Strauch et al., 2019). In contrast, recent tools implement exact optimization techniques, such as the R package *prioritizr* (Drever et al., 2025; Gopalakrishna et al., 2024; Hanson et al., 2025; Jung et al., 2021) via Mixed-Integer Linear Programming (MILP) (Alagador & Cerdeira, 2022; Billionnet, 2013). and the specifically restoration-focused R package *restoptr* via Constraint Programming (Justeau-Allaire et al., 2023; Deléglise et al., 2024). While heuristic methods are computationally

efficient for large-scale problems but may yield suboptimal outcomes, these exact methods guarantee optimal or near-optimal solutions at a higher computational cost (Beyer et al., 2016; Schuster et al., 2020).

Within exact optimization frameworks, ecological applications have used a variety of MOO formulations and solution strategies. These include weighted sum (Cheng et al., 2015; Lemos et al., 2023; López-Cubillos et al., 2022; Strassburg et al., 2018, 2020; Williams et al., 2020, 2024), lexicographic approaches (Geissler et al., 2025; Schuster et al., 2023), reference point methods (Deléglise et al., 2024; Dujardin & Chadès, 2018), maximin formulations (Cho et al., 2023; Martin et al., 2022; Palomo et al., 2019), and ε-constraint methods (Álvarez-Miranda et al., 2020; Cho & Sharma, 2020; Mazziotta et al., 2017), each offering different ways of reconciling competing goals (Williams & Kendall, 2017). Among these exact MOO techniques, Goal Programming (GP) is particularly well suited when objectives can be expressed as explicit target values. Rather than seeking trade-offs solely through relative objective weights, GP identifies compromise solutions by minimizing deviations from predefined aspiration levels (Williams & Kendall, 2017). This makes it appropriate for ecological planning problems in which policy thresholds, stakeholder expectations, or minimum acceptable levels of achievement must be incorporated within the optimization model. GP has been successfully applied in diverse ecological contexts, including the selection of forest conservation projects (Fooks & Messer, 2012), protected area management to foster stakeholder consensus (De Castro-Pardo & Azevedo, 2021), and the ranking of protected areas by integrating evolutionary and historical dimensions of biodiversity (Morales-Barbero & Ferrer-Castán, 2019). This flexibility positions GP as a promising approach for advancing restoration planning, providing a methodological basis for incorporating feasibility considerations alongside biodiversity and ecosystem service objectives.

This need is particularly relevant in the context of ambitious large-scale restoration initiatives (Eckert et al., 2023), such as Colombia's cost-effective restoration targets (Williams et al., 2024), India's integrative socio-ecological restoration planning (Gopalakrishna et al., 2024), and Canada's portfolio-based restoration approach (Drever et al., 2025). These examples illustrate growing efforts to extend SCP-based frameworks to large-scale, multi-criteria spatial restoration planning. However, despite these advances, few studies consider restoration feasibility as an explicit optimization objective. Existing approaches differ widely in how it is incorporated, ranging from GIS-based multicriteria screening without formal optimization (Orsi & Geneletti, 2010; Zamorano-Elgueta et al., 2025) to representation through operational proxies (e.g., minimizing distance to roads to improve access feasibility; Drever et al., 2025). These proxies primarily capture logistical considerations, reflecting a different facet of feasibility than that defined by exposure to recurrent ecological disturbance regimes.

To address this gap, we present a MOO framework grounded in SCP principles and formulated as a MILP model to guide large-scale spatial restoration prioritization. The framework simultaneously addresses four objectives—extinction risk reduction, carbon storage, water provision, and ecological restoration feasibility—under budget area and land suitability constraints. These objectives are reconciled using a GP approach. First, each objective is optimized independently to obtain single-objective benchmarks, capturing objective-specific

spatial configurations and providing target aspiration levels. These targets are then integrated into the GP model to generate balanced compromise solutions.

Unlike previous approaches where feasibility is treated as an external consideration—such as a hard constraint, screening criterion, or *post hoc* implementation filter—, our framework positions it as a competing objective within the optimization process. Feasibility is modeled as an ecological property reflecting the degree of exposure to disturbance regimes that affect restoration success. It is represented using spatial proxies—wildfire frequency, anthropogenic pressure, and invasive species richness—capturing a relative gradient of disturbance exposure across the landscape. In this formulation, higher feasibility values correspond to areas with lower exposure to these pressures and, consequently, a higher expected likelihood of long-term restoration success. The framework further enables a controlled comparison between multi-objective solutions obtained excluding and including feasibility, isolating its role in shaping spatial configurations and performance trade-offs. Beyond quantifying these trade-offs, the framework provides an interpretable view of the spatial configuration of restoration solutions, revealing the functional roles of planning units based on their relative selection frequency across optimization runs.

We apply this framework to continental Chile, which provides not only an exceptional ecological setting but also a compelling large-scale mathematical test case. Its extreme latitudinal and altitudinal gradients generate sharp spatial heterogeneity, leading to strong trade-offs among competing objectives and making it an ideal stress test for a multi-objective MILP framework. Chile harbors a unique biota characterized by exceptionally high levels of endemism (Scherson et al., 2014; Scherson et al., 2017; Fuentes-Castillo et al., 2019). This unique biodiversity is increasingly threatened by multiple anthropogenic pressures, including land-use change driven by urban expansion and productive activities such as agriculture, livestock farming, forestry, and mining, as well as pollution, exotic species invasions, wildfires, and resource extraction (Echeverría et al., 2006; Schulz et al., 2010; Vila et al., 2011; Miranda et al., 2015; Garreaud et al., 2019; Smith-Ramírez et al., 2021; Smith-Ramírez et al., 2022; Orrego et al., 2023; Garreaud et al., 2025). These interacting disturbances have led to extensive habitat loss and degradation, undermining biodiversity persistence and ecosystem service provision, and reinforcing the need for ecological restoration (Aronson et al., 2011; IUCN, 2022). In response, Chile has committed to international initiatives such as the Bonn Challenge and the 30×30 target of the Global Biodiversity Framework (CBD, 2022). Achieving these ambitious commitments, however, requires national-scale prioritization to identify where restoration actions can be allocated most effectively.

*Our contribution* The novelty of our framework lies not only in the selection of objectives but in how they are embedded and examined within the optimization structure. First, the framework designed as a controlled experimental setting in which all optimization runs share a common feasible region, while restoration feasibility is explicitly excluded or included as an objective. This design isolates the marginal effect of feasibility on spatial allocation and trade-offs, a capability lacking in existing MILP-based models where feasibility is either imposed as a constraint or incorporated *ex post*. Second, by combining GP with diagnostics based on selection frequency, the framework provides an interpretable view of compromise solutions. Rather than reducing multi-objective

outcomes to undifferentiated balances, this approach reveals how trade-offs in objective space translate into differentiated functional roles in geographic space, distinguishing multipurpose, objective-specific, and balance-supporting planning units. Together, these features extend MILP-based SCP models from tools that merely identify efficient solutions to frameworks that explicitly explain the structural logic underlying those solutions.

## 2. Methods

### 2.1. Overview of the optimization framework

We formulated a multi-objective optimization framework as a mixed-integer linear programming model to support spatial restoration planning. The framework integrates four criteria linked to distinct ecological and socio-environmental objectives: reducing species extinction risk (biodiversity conservation), restoring and protecting carbon storage (climate change mitigation), improving water provision (streamflow and water quality), and enhancing restoration feasibility (likelihood of long-term restoration success from an ecological perspective). Throughout the paper, we use the term *objective* to refer to overarching planning goals and *criterion* to denote the specific measurable quantities optimized in the model; where no ambiguity arises, both terms are used interchangeably.

The framework was implemented in two steps. First, each criterion was optimized independently to establish benchmark solutions. Second, the criteria were optimized jointly using a goal programming approach, with single-objective outcomes serving as reference targets. To isolate the role of restoration feasibility, we compared two multi-objective formulations that share an identical feasible region and constraint structure, differing only in whether feasibility is included as an optimization objective. This design enables a controlled assessment of the marginal effect of incorporating feasibility on spatial allocation patterns, trade-offs among objectives, and overall solution performance under a fixed restoration area budget and land suitability constraints. Beyond trade-off analysis, we examined the spatial configuration of solutions using an irreplaceability proxy defined as the frequency with which a unit is selected across optimization runs (Pressey et al., 1993, 1994; Ferrier et al., 2000), allowing the identification of multipurpose, objective-specific, and balance-supporting components. All optimization runs were conducted under a common set of constraints representing limited restoration capacity and ecological suitability, ensuring that differences among solutions reflect interactions among objectives rather than changes in feasibility conditions.

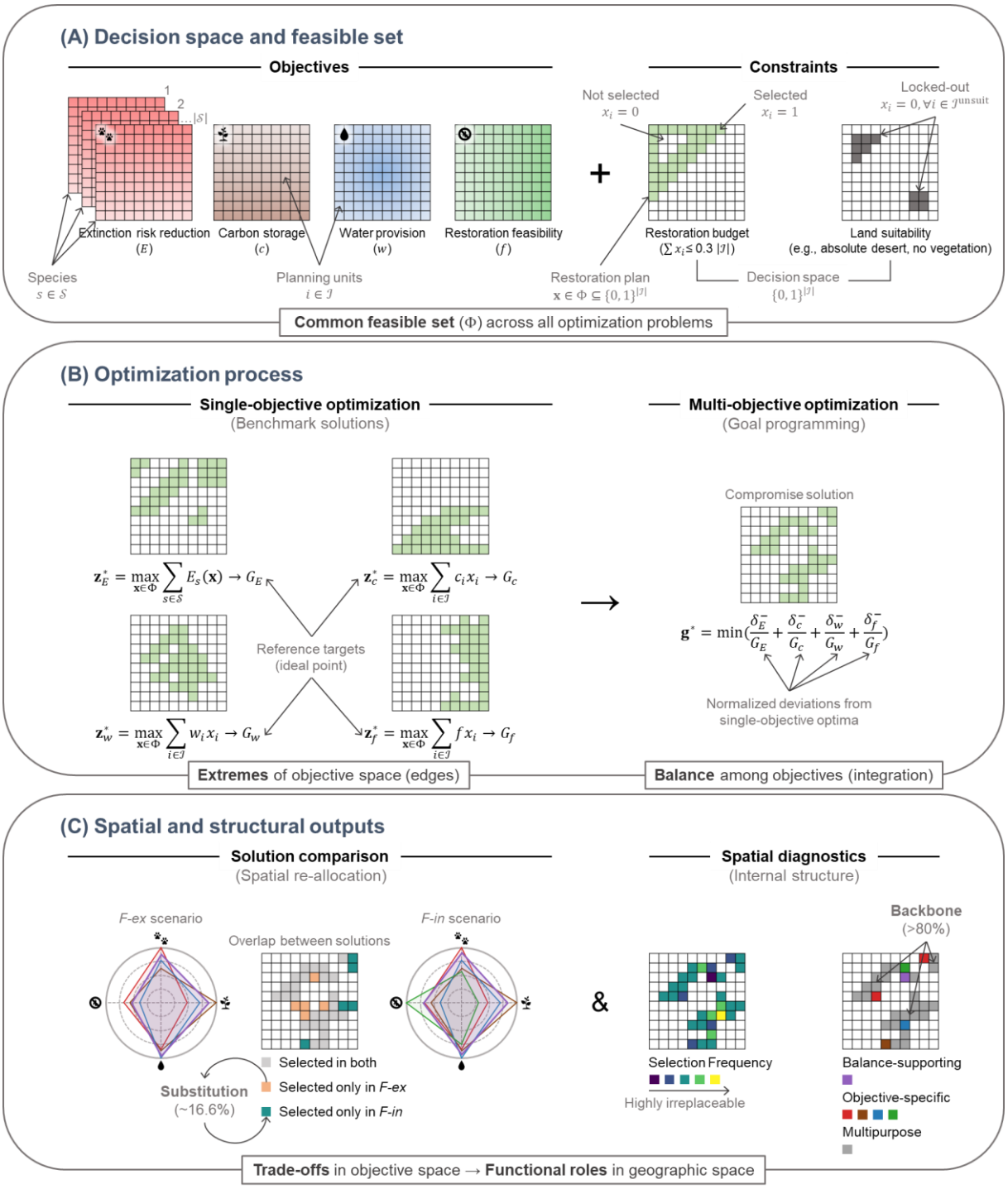


**Fig. 1 | Conceptual scheme of the optimization framework, experimental design, and diagnostic outputs.** This figure summarizes the structure of the multi-objective restoration framework. **(A) Decision space and feasible region**, where spatial features associated with extinction risk reduction ($E$), carbon storage ($c$), water provision ($w$), and restoration feasibility ($f$) are integrated with a fixed restoration budget of 30% and land suitability constraints (e.g., excluding units corresponding to non-restorable land-cover types such as water bodies, wetlands and glaciers/snow). **(B) Optimization process**, illustrating the two-step formulation. Single-objective solutions first yield benchmark optima ($\mathbf{z}_E^*$, $\mathbf{z}_c^*$, $\mathbf{z}_w^*$, $\mathbf{z}_f^*$),

which define the reference targets used in the goal programming model ($G_E = \mathbf{z}_E^*$, $G_c = \mathbf{z}_c^*$, $G_w = \mathbf{z}_w^*$, $G_f = \mathbf{z}_f^*$). The multi-objective solution ($\mathbf{g}^*$) is then obtained by minimizing normalized deviations from these targets, ensuring scale-invariant integration across criteria. **(C) Spatial and structural outputs**, used to evaluate model results. Solution comparison quantifies spatial reallocation among scenarios, isolating the effect of explicitly including restoration feasibility. Spatial diagnostics classify units according to their consistency of selection across optimization problems, distinguishing multipurpose, objective-specific, and balance-supporting components of the compromise solution.

*Notation and preliminaries* The optimization framework is defined over a common set of spatial planning units (hereafter, *units*), which represent the elementary decision units over which restoration actions can be spatially allocated. Let $\mathcal{I}$ denote the set of units, indexed by $i$. For each unit $i \in \mathcal{I}$, we define a binary decision variable $x_i \in \{0, 1\}$ where $x_i = 1$ indicates that unit $i$ is selected for restoration and $x_i = 0$ otherwise. Collectively, these variables define a restoration plan $\mathbf{x} = (x_i)_{i \in \mathcal{I}} \in \{0, 1\}^{|\mathcal{I}|}$. All objectives and constraints are formulated over this common decision space. The full mathematical formulation of the framework is provided in Appendix A (Supplementary Material).

## 2.2. Study region

We applied the framework to continental Chile as a case study to illustrate its performance under a complex, large-scale, and ecologically heterogeneous setting. Continental Chile spans latitudes 17°29′57″ S to 56°32′12″ S and encompasses strong climatic, biogeographic, and ecological gradients shaped by its latitudinal extent, the Pacific Ocean to the west, and the Andes Mountains to the east. It covers 746,303.43 km² and includes 19 vegetation formations and 125 terrestrial ecosystems (Luebert & Pliscoff, 2017; Pliscoff et al., 2025).

Over half of these terrestrial ecosystems have undergone degradation or transformation since colonization, driven by agriculture, forestry, urbanization, livestock grazing, mining, wildfires, and biological invasions (Orrego et al., 2022). Currently, 79.2% of terrestrial ecosystems are classified as Critically Endangered, Endangered, Vulnerable, or Near Threatened (Pliscoff et al., 2025), making Chile a demanding test case for large-scale spatial restoration prioritization.

The study area was discretized into a regular grid of resolution 1 km$^2$ (1 km × 1 km), resulting in 812,910 units across continental Chile. All spatial input datasets were harmonized to this resolution and projected onto a common coordinate reference system (WGS84 / UTM Zone 19S) prior to analysis. Units intersecting coastlines and territorial boundaries may represent smaller land areas, explaining the difference between the total number of units and the reported land surface. This resolution provides a balance between computational tractability and spatial detail appropriate for national-scale planning. More generally, the framework is resolution-independent and can be applied at finer or coarser spatial scales, as well as in different geographic contexts.

This discretization defines the set of planning units $\mathcal{I}$, while the feasible set of restoration plans is determined by the constraints described below.

## 2.3. Restoration budget and land suitability constraints

The optimization framework incorporated two generic constraints common to spatial restoration planning: a *restoration budget constraint* and a *land suitability constraint*. Together, these constraints define the feasible set of restoration plans, denoted by $\Phi \subseteq \{0,1\}^{|\mathcal{I}|}$, consisting of all decision vectors $\mathbf{x}$ that satisfy both the restoration budget and land suitability constraints. All optimization problems in the framework were solved over this common feasible set $\Phi$.

We imposed an area-based restoration budget that limited the total area selected for restoration. Let $a_i$ denote the area of unit $i$ (1 km$^2$), and let $A = \sum_{i \in \mathcal{I}} a_i$ denote the total area of the study region. Let $t_A \in (0,1]$ represent the proportion of the total area available for restoration. The budget constraint is defined as:

$$\sum_{i \in \mathcal{I}} a_i x_i \leq t_A A \qquad \text{Eq. (1)}$$

which restricted the total selected area to a fixed fraction of the landscape. This formulation avoids introducing explicit cost heterogeneity when restoration costs are assumed proportional to area, while remaining general enough to accommodate heterogeneous costs or alternative budget definitions if required.

To ensure ecological consistency, the framework excluded units incompatible with restoration based on a land suitability mask derived from biophysical constraints. Specifically, $\mathcal{I}^{\text{unsuit}} \subseteq \mathcal{I}$ denotes the set of units classified as non-restorable (e.g., areas lacking vegetation or exhibiting conditions that preclude ecological recovery). Land suitability is enforced through an exclusion (locked-out) constraint:

$$x_i = 0, \qquad \forall i \in \mathcal{I}^{\text{unsuit}} \qquad \text{Eq. (2)}$$

which restricts the optimization to ecologically restorable areas. This constraint ensures that restoration actions are allocated only to suitable locations, while allowing the specific definition of suitability to vary across datasets, ecosystem classifications, or restoration objectives.

**Case study parameterization.** For the Chilean case study, we set $t_A = 0.3$, consistent with Target 2 of the Kunming–Montreal Global Biodiversity Framework. Under the uniform grid resolution ($a_i = 1\ km^2$ for all units), the total area satisfies $A = |\mathcal{I}|$, and Eq. (1) simplifies to $\sum_{i \in \mathcal{I}} x_i \leq 0.3|\mathcal{I}|$, which effectively limits the total number of selected units to 30% of the national territory.

Land suitability was defined using national land cover and ecosystem datasets, as detailed below. Units classified as wetlands, water bodies, primary and secondary forests, impervious surfaces, salt flats, ice, and snow were excluded based on land cover information (Zhao et al., 2016), as they either correspond to ecosystems that maintain natural ecological functions or to areas where ecological restoration is not feasible. Accordingly, the analysis focused on terrestrial land-cover types with restoration potential, including croplands, forest plantations, grasslands, shrublands, and bare lands.

In addition, areas classified as absolute desert were excluded based on the national terrestrial ecosystems classification for Chile (Pliscoff et al., 2025), as they lack vegetation and the model assumes recovery through

natural or assisted regeneration. Together, these criteria define the set of units eligible for restoration in the Chilean case study.

## 2.4. Step 1: Single-objective optimization

Each criterion—extinction risk reduction, carbon storage, water provision, and restoration feasibility—was optimized independently over the common feasible set Φ. This step establishes a reference system in objective space by identifying the best achievable performance for each criterion when considered in isolation.

The resulting optimal values ($\mathbf{z}_j^*$) define the *ideal point*, which represents the upper bound of achievable outcomes across all objectives under the given budget and suitability constraints. Because criteria are optimized separately, the ideal point is generally not jointly reachable, reflecting the inherent trade-offs among competing objectives in the Chilean landscape.

These single-objective solutions fulfill two complementary purposes. First, they provide aspiration levels (benchmark values) that are subsequently used as reference targets in the multi-objective goal programming formulation (Step 2). Second, they offer a basis for interpreting trade-offs by revealing how prioritizing one objective affects the performance of others within the same feasible decision space.

### 2.4.1. Extinction risk reduction: biodiversity conservation

We quantified biodiversity conservation benefits as the reduction in species extinction risk resulting from the spatial allocation of restoration actions. Extinction risk was modeled using a species–area relationship (SAR), which links changes in habitat area to the probability of species extinction (Thomas et al., 2004). This formulation allows extinction risk to be expressed as a function of habitat loss and recovery, making it suitable for integration within spatial optimization frameworks.

Let $\mathcal{S}$ denote the set of species, indexed by $s$. We define the baseline species–area ratio as:

$$q_s^0 = \frac{a_s^0}{A_s^0}$$

where $a_s^0$ is the current habitat area of species $s$, $A_s^0$ is its original (e.g., pre-settlement) habitat area.

Under a restoration plan $\mathbf{x} \in \Phi$, projected species–area ratio is defined as:

$$q_s(\mathbf{x}) = \frac{a_s^0 + a_s(\mathbf{x})}{A_s^0}$$

where $a_s(\mathbf{x})$ denotes the total increase in habitat area for species $s$ resulting from restoration across selected units. Because $a_s^0 + a_s(\mathbf{x})$ can exceed the species' reference area $A_s^0$, the ratio may exceed 1. This ensures that $q_s(\mathbf{x}) \in [0, 1]$, preserving its ecological interpretation as a proportion of reference habitat.

Extinction risk is then defined as a function of the species–area ratio. The baseline extinction risk of species $s$, denoted $e_s^0$, and the projected extinction risk under restoration plan $\mathbf{x}$, denoted $e_s(\mathbf{x})$, are given by:

$$e_s^0 = 1 - (q_s^0)^{\alpha}, \qquad e_s(\mathbf{x}) = 1 - \left(q_s(\mathbf{x})\right)^{\alpha}$$

where $\alpha \in (0, 1]$ is the species–area exponent controlling how extinction risk increases as habitat is lost. By construction, extinction risk values lie within the interval $[0, 1]$, where $e_s(\mathbf{x}) = 0$ corresponds to no extinction risk and $e_s(\mathbf{x}) = 1$ to complete extinction, preserving the ecological interpretation of the metric.

The corresponding reduction in extinction risk for species $s$ under restoration plan $\mathbf{x}$ is defined as:

$$E_s(\mathbf{x}) = e_s^0 - e_s(\mathbf{x})$$

which captures the ecological benefit of restoration in terms of risk mitigation. The biodiversity conservation objective is then defined as:

$$\mathbf{z}_E^* = \max_{\mathbf{x} \in \Phi} \sum_{s \in S} E_s(\mathbf{x}) \qquad \text{Eq. (3)}$$

Because the species–area relationship is nonlinear, it was approximated using a piecewise-linear (PWL) representation to preserve linearity and computational tractability within the MILP framework. Specifically, the function $\left(q_s(\mathbf{x})\right)^{\alpha}$ is approximated over the relevant domain of $q_s(\mathbf{x})$ using a set of breakpoints and linear segments, following the extinction risk formulation and PWL linearization strategy implemented by Moreno-Faguett et al. (2026). The approximation tolerance is controlled through an adaptive breakpoint construction procedure (see Appendix A, Section A.4). This approximation affects only the numerical evaluation of extinction risk and does not alter the underlying feasible decision space or optimization structure.

**Case study parameterization.** For the Chilean case study, we parameterized this objective using spatially explicit habitat information for threatened flora and fauna species. We considered 154 threatened terrestrial species (refer to Table S1 in the Supplementary Material for the full list of species).

- *Current habitat maps* ($a_s^0$). Current habitat distributions were derived from species distribution models (SDMs) developed using occurrence records obtained from GBIF (GBIF.org, 2024a,b) and not-correlated selection of bioclimatic variables (bio1, bio4, bio5, bio6, bio12, bio15, and bio16; Pliscoff et al., 2014). SDMs were generated using MaxEnt with a random test percentage of 30%, a maximum of 1,000 iterations, and the "maximum training sensitivity plus specificity" threshold rule to produce binary presence–absence maps.
- *Pre-settlement habitat maps* ($A_s^0$). Pre-settlement habitat distributions were reconstructed using data from the Chilean Ministry of the Environment (https://simbio.mma.gob.cl/), which associates native species with terrestrial ecosystems. These associations were combined with the pre-settlement potential terrestrial ecosystems map for Chile (Luebert & Pliscoff, 2017) to delineate the original habitat area $A_s^0$ for each species.

For each unit $i$, the contribution to species $s$ was quantified by $a_{is}$, defined as the area (km$^2$) of unit $i$ overlapping the habitat of species $s$. These values determine the species-specific gains under restoration through:

$$a_s(\mathbf{x}) = \sum_{i \in \mathcal{I}} a_{is} x_i$$

Following Thomas et al. (2004), we set the species–area exponent to $\alpha = 0.25$, a commonly used value for estimating extinction risk from habitat loss and one that ensures consistency with previous conservation planning studies (e.g., Strassburg et al., 2018).

**2.4.2. Carbon storage: climate change mitigation**

We quantified climate change mitigation benefits as the enhancement and retention of carbon stocks through the spatial prioritization of restoration actions. Carbon storage was represented as a spatially explicit carbon stock assigned to each unit, reflecting the amount of carbon that can be retained under restoration. Carbon storage was treated as a proxy for the potential climate mitigation benefit of restoration, assuming that areas with higher existing carbon stocks provide greater benefits through retention and avoided loss. Accordingly, restoration actions were assumed to maintain or enhance current carbon stocks rather than explicitly modeling dynamic post-restoration carbon accumulation.

The climate mitigation objective is defined as:

$$\mathbf{z}_c^* = \max_{\mathbf{x} \in \Phi} \sum_{i \in \mathcal{I}} c_i x_i \qquad \text{Eq. (4)}$$

where $c_i$ denotes the total carbon stock associated with unit $i$.

This linear formulation ensures compatibility with the MILP framework, enabling joint optimization with other criteria within the feasible set Φ. This property applies not only to the present objective but also to the remaining objective functions defined below. At the same time, the linear structure provides a simple and flexible representation that can be adapted to alternative data sources without modifying the underlying optimization framework.

**Case study parameterization.** For the Chilean case study, carbon storage was quantified by combining soil organic carbon and above-ground biomass carbon stocks at the planning-unit level.

- *Soil carbon stock*. Soil organic carbon data were obtained from the Global Soil Organic Carbon Map v1.5 (GSOC), corresponding to the year 2019 (FAO & ITPS, 2020).
- *Above-ground biomass carbon stock*. Above-ground biomass data were obtained from the ESA Biomass Climate Change Initiative, which provides global datasets of above-ground biomass for multiple years (Santoro & Cartus, 2024). We used the most recent available dataset, corresponding to the year 2021.

For each unit, total carbon stock $c_i$ was computed as the sum of soil organic carbon and above-ground biomass carbon, expressed in consistent units prior to optimization.

### 2.4.3. Water provision: streamflow and water quality

We quantified hydrological benefits related to streamflow regulation and water quality by prioritizing restoration actions in areas hydrologically connected to riparian ecosystems. Riparian vegetation contributes to hydrological regulation by enhancing infiltration, moderating runoff, and reducing sediment and nutrient loads, thereby supporting both streamflow stability and water quality (Lara et al., 2009; Little et al., 2015).

To represent these effects in a spatially explicit yet computationally tractable manner, water provision was operationalized using a distance-based riparian proxy. This proxy serves as a simplified indicator of the potential influence of restoration on hydrological processes, rather than as a process-based hydrological model. Under this formulation, each unit was assigned a water provision weight $w_i$, reflecting the decline in riparian influence with increasing distance from surface water. This formulation assumes that restoration actions in these ecosystems enhance hydrological regulation and water quality, consistent with evidence that riparian vegetation plays a key role in mediating runoff, sediment retention, and nutrient filtering (e.g., Lara et al., 2009; Little et al., 2015).

The streamflow and water quality objective is defined as:

$$\mathbf{z}_w^* = \max_{\mathbf{x}\in\Phi} \sum_{i\in\mathcal{I}} w_i x_i \qquad \text{Eq. (5)}$$

where $w_i$ represents the priority value assigned to unit $i$ based on proximity to riparian ecosystems.

**Case study parameterization.** For the Chilean case study, water-related priority values were derived from national hydrological datasets. Vector layers of the hydrographic network and water bodies were obtained from the Geospatial Data Infrastructure Platform of Chile (https://www.ide.cl/).

Riparian influence was operationalized by applying a 1 km buffer on either side of mapped watercourses and water bodies. This distance does not represent a strict ecological threshold, but rather reflects the spatial resolution of the planning units (1 km$^2$) and ensures consistent integration of riparian influence within the optimization framework. Units intersecting this buffer were assigned the maximum priority value ($w_i = 1$), while priority values for units outside the buffer decreased with distance from surface water.

Euclidean distances to the nearest watercourse or water body were calculated and transformed into priority values through an inverted min–max normalization, producing a linearly rescaled distance-decay function defined over the interval $[0, 1]$, such that priority decreases proportionally with increasing distance. The resulting raster layer was then aggregated to the unit level prior to optimization.

### 2.4.4. Restoration feasibility: likelihood of long-term restoration success

We quantified restoration feasibility as a composite measure reflecting the likelihood that restoration actions will succeed and persist over the long term. This definition aligns with an ecological interpretation of feasibility grounded in exposure to recurrent disturbance regimes, rather than feasibility defined in economic or logistical terms. Following the conceptual approach proposed by Orsi and Geneletti (2010), feasibility was represented using spatial proxies capturing biophysical and anthropogenic factors known to influence restoration outcomes.

Restoration feasibility was expressed as a unit-specific index $f_i$, constructed from standardized components representing distinct dimensions of feasibility. Higher values of $f_i$ indicate locations with more favorable ecological conditions for restoration, implying greater likelihood of success, long-term persistence, and reduced need for post-restoration interventions.

In this framework, restoration is conceptualized at broad spatial scales as assisted ecological recovery, where natural regeneration is facilitated through targeted, low-intensity interventions, particularly in modified landscapes such as pastures and croplands. This approach assumes that reducing key pressures and prioritizing ecologically feasible landscapes increases the likelihood of sustained recovery. Accordingly, the feasibility index captures key landscape-level constraints on vegetation regeneration, rather than the full ecological complexity of recovery processes, under the premise that restoration success increases where pressures are lower and conditions favor assisted natural regeneration.

The restoration feasibility objective is defined as:

$$\mathbf{z}_f^* = \max_{\mathbf{x}\in\Phi} \sum_{i\in\mathcal{I}} f_i x_i \qquad \text{Eq. (6)}$$

where $f_i$ denotes the composite feasibility score associated with unit $i$.

**Case study parameterization.** For the Chilean case study, restoration feasibility was operationalized using three spatial proxies capturing fire frequency, anthropogenic pressure, and invasive species richness.

- *Fire disturbance* ($d_i^{\text{fire}}$), represented as the distance from unit $i$ to areas that experienced two or more wildfires during the past decade. Greater distance from recurrently burned areas reflects lower soil degradation and reduced likelihood of fire recurrence, increasing restoration feasibility (Tessler et al., 2016; Smith-Ramírez et al., 2021). Fire history data were obtained from large-scale wildfire records provided by the National Forest Corporation of Chile (CONAF) for the period 2013–2023. Pixels with two or more recorded fires were identified and used as the reference layer for distance calculations.
- *Anthropogenic disturbance* ($d_i^{\text{anth}}$), represented as the distance from unit $i$ to roads and human infrastructure, based on the national road network and building footprints derived from Google's Open Buildings dataset (Sirko et al. 2021). This dataset provides spatially explicit building polygons generated from high-resolution satellite imagery using deep learning models. Greater distances indicate lower exposure to human pressures that may compromise restoration persistence (Altamirano et al., 2013; Úbeda & Sarricolea, 2016).

- *Invasive species disturbance* ($d_i^{\text{inv}}$), represented as the inverse of invasive species richness within unit $i$. Areas with lower invasive pressure were considered more feasible for restoration, as they typically require lower investment in invasive species control (Vargas-Ríos et al., 2014). Invasive species richness was estimated using ensemble species distribution models for naturalized invasive species with more than 100 occurrence records in continental Chile and projected to expand their potential distribution by at least 30% by 2040 (refer to Table S2 in the Supplementary Material for the full list of species). For each species, ensemble models were generated using biomod2 (Thuiller et al. 2009; 2016), combining predictions from multiple algorithms under current and future climatic conditions. Continuous suitability outputs were transformed into binary maps of potential presence using a fixed suitability threshold of 0.7, and then spatially aggregated to estimate the potential richness of invasive species within each planning unit (Fuentes-Lillo, 2024).

Each proxy was standardized to the interval $[0, 1]$ and combined using an additive aggregation scheme to produce a composite feasibility index:

$$f_i = \frac{d_i^{\text{fire}} + d_i^{\text{anth}} + d_i^{\text{inv}}}{3}, \qquad \forall i \in \mathcal{I}$$

All components were assigned equal importance, implicitly assuming comparable contributions of each disturbance dimension to restoration feasibility. This choice provides a transparent and consistent baseline while avoiding the introduction of subjective weights that could bias prioritization outcomes.

This index was used in the optimization to prioritize units less exposed to recurrent fires, human disturbance, and invasive species pressure, thereby increasing the likelihood of successful and sustained restoration outcomes.

## 2.5. Step 2: Multi-objective optimization

The multi-objective problem builds directly on the results of Step 1, where single-objective optimizations were used to define the ideal point. Using these reference values, we formulated a normalized goal programming model to identify a compromise solution that minimizes proportional deviations from the single-objective optima across competing criteria.

Let $\mathcal{J} = \{E, c, w, f\}$ denote the set of optimization criteria, corresponding to extinction risk reduction, carbon storage, water provision, and restoration feasibility, respectively. For each criterion $j \in \mathcal{J}$, a target value $G_j$ is defined as the optimal value obtained from the corresponding single-objective optimization (Step 1), that is,

$$G_j = \mathbf{z}_j^*$$

where $\mathbf{z}_j^*$ denotes the optimal objective value of criterion $j$ as defined in Eqs. (3)–(6). Collectively, the targets $\{G_j\}_{j\in\mathcal{J}}$ define the ideal point $(\mathbf{z}_E^*, \mathbf{z}_c^*, \mathbf{z}_w^*, \mathbf{z}_f^*)$ in objective space.

Let $b_j(\mathbf{x})$ denote the value achieved by criterion $j$ under a restoration plan $\mathbf{x} \in \Phi$, computed using the same expressions as in the corresponding single-objective formulation (**Section 2.4**). Specifically,

$$b_E(\mathbf{x}) = \sum_{s \in \mathcal{S}} \left(e_s^0 - e_s(\mathbf{x})\right), \qquad b_c(\mathbf{x}) = \sum_{i \in \mathcal{I}} c_i x_i, \qquad b_w(\mathbf{x}) = \sum_{i \in \mathcal{I}} w_i x_i, \qquad b_f(\mathbf{x}) = \sum_{i \in \mathcal{I}} f_i x_i$$

Deviations from each reference target were captured using non-negative deviation variables $\delta_j^+$ (*overachievement*) and $\delta_j^-$ (*underachievement*), enforced through the goal constraint:

$$b_j(\mathbf{x}) - \delta_j^+ + \delta_j^- = G_j, \qquad \forall j \in \mathcal{J}. \qquad \text{Eq. (7)}$$

In its general form, the GP problem is formulated as:

$$\mathbf{g}^* = \min_{\mathbf{x} \in \Phi} \sum_{j \in \mathcal{J}} \omega_j \left( \frac{\delta_j^+ + \delta_j^-}{G_j} \right)$$

where $\omega_j$ are criterion-specific weights reflecting the relative importance assigned to each objective. Normalization by $G_j$ ensures scale invariance, allowing direct comparison across heterogeneous criteria by expressing deviations in proportional terms.

Because each target $G_j$ corresponds to the maximum achievable value of criterion $j$ over the feasible set $\Phi$, it follows that $b_j(\mathbf{x}) \leq G_j$ for any feasible solution $\mathbf{x} \in \Phi$. Consequently, overachievement is not possible and $\delta_j^+ = 0$ for all $j \in \mathcal{J}$. The formulation therefore simplifies to:

$$\mathbf{g}^* = \min_{\mathbf{x} \in \Phi} \sum_{j \in \mathcal{J}} \frac{\delta_j^-}{G_j} \qquad \text{Eq. (8)}$$

which minimizes the normalized shortfall from each target across all criteria, subject to the constraints defining the feasible set $\Phi$ (i.e., restoration budget and land suitability constraints; see **Section 2.3**), together with the goal constraints in Eq. (7). All weights were set to unity ($\omega_j = 1$), providing a neutral baseline that avoids introducing subjective preference biases and allows isolating the effect of explicitly incorporating restoration feasibility into the optimization.

This formulation is equivalent to minimizing the L1-distance to the ideal point in normalized objective space. It thus identifies a balanced compromise solution that approaches each criterion as closely as possible in relative terms, without privileging any single objective. In this sense, GP acts as a synthesis mechanism that explicitly captures trade-offs among competing objectives while maintaining a transparent link between objective-space performance and the resulting spatial configuration of restoration actions.

## 2.6. Solution comparison and spatial diagnostics

To isolate the effect of including restoration feasibility in the multi-objective formulation, we solved two GP scenarios that differed only in their set of optimization criteria: a *feasibility-excluded* scenario (F-ex), which considered biodiversity conservation, carbon storage, and water provision, defined over the set $\mathcal{J}^{\mathrm{F-ex}} =$

$\{E, c, w\}$, and a *feasibility-included* scenario (F-in), which incorporated restoration feasibility as an explicit objective, defined over the set $\mathcal{J}^{\mathrm{F-in}} = \{E, c, w, f\}$.

Because both scenarios share the same feasible set Φ and GP formulation, differences between the resulting solutions reflect the inclusion of feasibility as an explicit objective. This design enabled a controlled assessment of how feasibility modifies spatial allocation patterns, trade-offs among objectives, and the overall performance of solutions under fixed spatial constraints.

In both scenarios, the GP formulation minimizes normalized shortfalls from the corresponding single-objective benchmarks over the relevant set of criteria $\mathcal{J}^{\mathrm{F-ex}}$ or $\mathcal{J}^{\mathrm{F-in}}$, yielding compromise solutions that balance biodiversity conservation, ecosystem services, and, where applicable, restoration feasibility. Comparisons between F-ex and F-in solutions were conducted in both objective space and geographic space to distinguish objective-level performance differences from spatial re-allocation.

Finally, to characterize the internal composition of the F-in solution, we computed an *ex post* irreplaceability proxy based on the frequency with which each unit is selected across optimization runs. Let $\mathcal{R}$ denote the set of five optimization runs considered (including the four single-objective benchmarks and the multi-objective F-in solution), and let $x_i^{(r)}$ denote the selection of unit $i$ in run $r$. The selection frequency of unit $i$ is defined as:

$$\rho_i = \sum_{r \in \mathcal{R}} x_i^{(r)}.$$

which corresponds to the number of optimization runs in which unit $i$ is selected. This metric reflects how consistently units contribute across optimization problems, enabling their classification into distinct *functional roles* within the compromise solution. Specifically, we define these roles as follows: *multipurpose* units, which contribute simultaneously to multiple individual objectives; *objective-specific* units, which are prioritized primarily for a single goal; and *balance-supporting* units, which emerge exclusively in the multi-objective framework to negotiate trade-offs among competing criteria.

## 3. Results

*Experimental setting* All optimization experiments were solved using Gurobi Optimizer v11.0.2 (win64) on Windows 10 on an 11th Gen Intel(R) Core(TM) i7-1165G7 @ 2.80 GHz workstation (4 physical cores, 8 logical processors), using up to 8 threads. A relative optimality tolerance of MIPGap = 0.01 (1%) was enforced for all runs, with default values used for all remaining parameters (no time limit). All reported solutions satisfied the imposed tolerance, achieving final optimality gaps below 0.001%. Despite the large problem size (over 800,000 units), optimization runs were solved within approximately 20 to 700 s. When considering the full end-to-end workflow—including preprocessing, model construction, optimization, and post-processing—the total pipeline runtime averaged 1,440 s across experiments (≈24 minutes). Further computational details are provided in Table B1 and Appendix B.

### 3.1. Spatial patterns of single-objective solutions

Figure 2 presents the spatial distribution of units selected under each single-objective optimization, together with the corresponding latitudinal profiles. The configuration of selected units varied across objectives, showing that each criterion produced distinct allocation patterns along continental Chile. Although all solutions selected the same total number of units under the fixed area budget, their latitudinal distributions differed markedly among objectives.

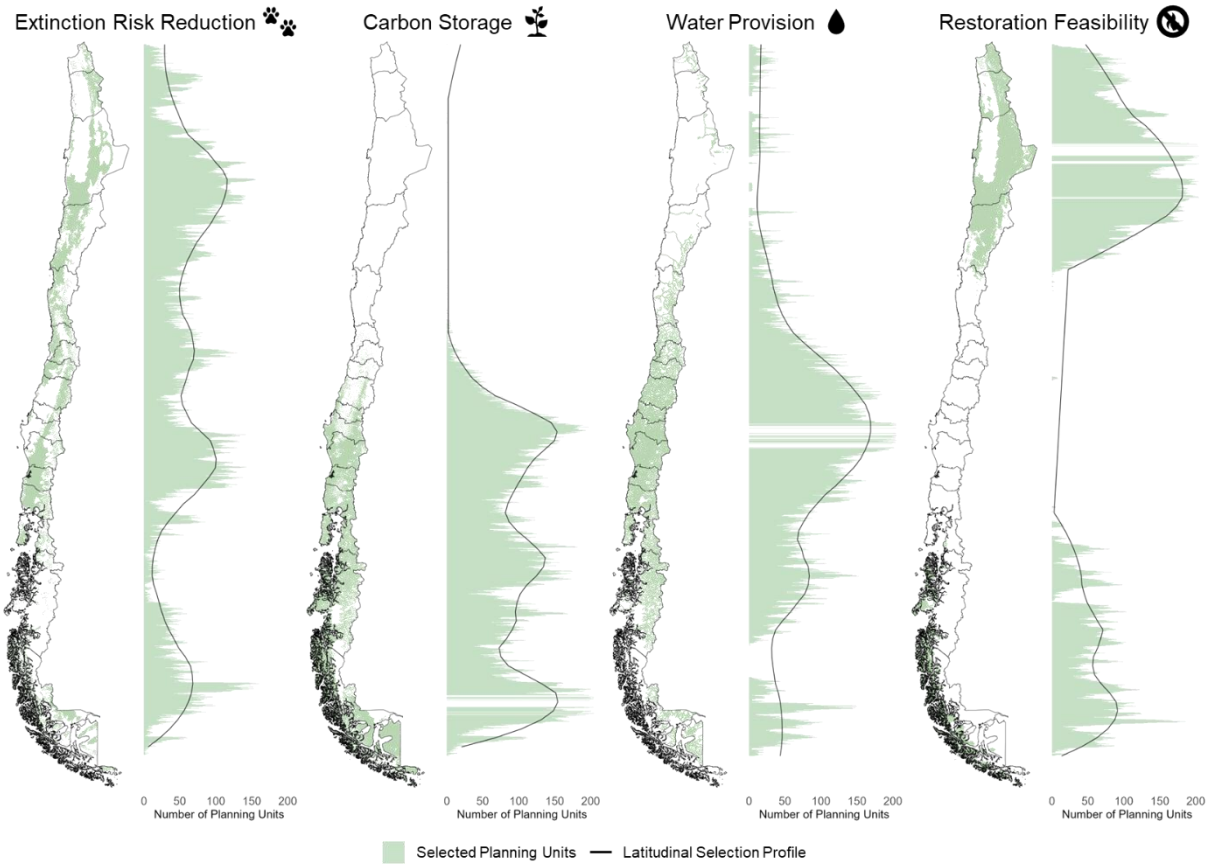


**Fig. 2 | Spatial distribution of selected planning units in single-objective optimization solutions across continental Chile.** Each panel displays the spatial allocation of restoration priorities (maps) and their corresponding latitudinal selection profiles for the four primary objectives: extinction risk reduction, carbon storage, water provision, and restoration feasibility. Light green areas denote selected planning units, while the adjacent profiles depict the number of units selected per 1-km latitudinal band (bars) along with a smoothed latitudinal selection trend (black line). Distinct spatial signatures and restoration hotspots emerge for each objective, reflecting the contrasting geographic distribution of their underlying ecological and environmental drivers.

These contrasts are reflected in the latitudinal profiles (Fig. 2, right panels). Carbon storage and restoration feasibility exhibited more concentrated patterns, with higher mean numbers of selected units per latitudinal band (92.8 ± 54.0 and 87.9 ± 57.4 units, respectively; Table C1). In contrast, extinction risk reduction and water

provision displayed flatter profiles, characterized by lower mean counts per band (57.3 ± 35.6 and 68.3 ± 55.7 units, respectively), consistent with a more spatially dispersed allocation along the latitudinal gradient.

Variability across latitude also differed among objectives (see CV and IQR [25–75%] in Table C1). Water provision showed the highest relative dispersion (CV = 0.816; IQR = 22–105 units), whereas carbon storage exhibited a more even distribution across bands (CV = 0.582; IQR = 57–130), despite pronounced absolute peaks. Restoration feasibility presented intermediate variability (CV = 0.653; IQR = 47–118), while extinction risk reduction combined lower overall counts with moderate variability (CV = 0.622; IQR = 30–80), resulting in smoother profiles with fewer extreme concentrations. Together, these patterns show that each single-objective solution emphasized different latitudinal zones, generating objective-specific spatial signatures that served as a baseline for comparison with multi-objective compromise solutions (F-ex and F-in).

### 3.2. Effects of restoration feasibility in multi-objective optimization

As shown in Fig. 3, the multi-objective solutions obtained excluding (F-ex) and including (F-in) restoration feasibility selected the same total number of units but differed in spatial allocation. Of the selected units, 203,594 were shared by both solutions, whereas 40,279 units were exchanged between them, reflecting spatial substitutions under the same area constraints.

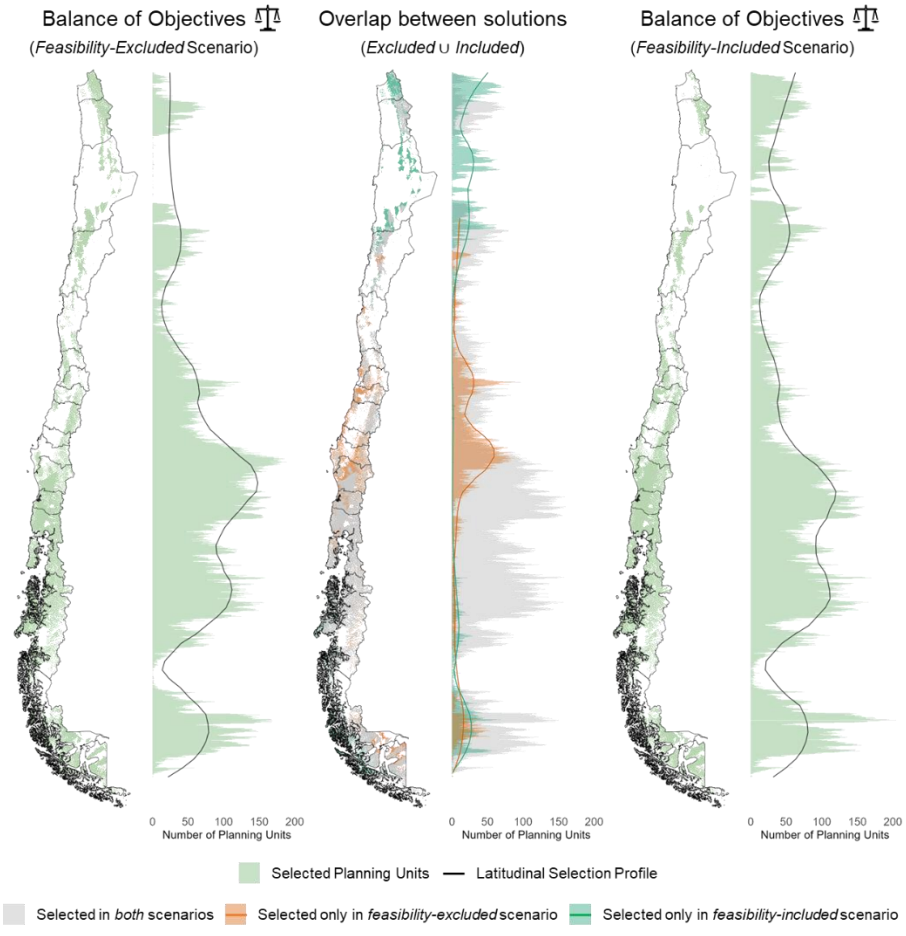

**Fig. 3 | Spatial comparison between multi-objective solutions obtained excluding and including restoration feasibility.** Left and right panels show the compromise solutions (Balance of Objectives) excluding (F-ex) and including (F-in) feasibility, respectively. The central panel displays their spatial overlap and differences, where gray denotes units selected in both solutions, orange indicates units selected only when feasibility is excluded, and turquoise indicates units selected only when feasibility is included. Adjacent latitudinal profiles depict the absolute number of selected units per 1-km latitudinal band, highlighting how the explicit inclusion of feasibility reshapes latitudinal coverage and drives spatial redistribution across continental Chile.

Common units (gray in Fig. 3) formed a shared spatial backbone, while non-overlapping units (orange and turquoise) were interspersed across the study area rather than being concentrated in a single region. These differences reflect alternative spatial configurations achieving comparable objective performance under the same area constraint.

Latitudinal profiles in Fig. 3 summarize how substitutions were distributed along the north–south gradient. In the F-ex scenario, selected units spanned 3,820 latitudinal bands, whereas including feasibility extended coverage to 4,150 bands (Table C1). This shift corresponded to a lower mean number of selected units per band ($58.8 \pm 41.7$ in F-in vs. $63.8 \pm 46.9$ in F-ex) and a slight reduction in relative dispersion (CV = 0.710 vs. 0.735), consistent with a broader latitudinal spread.

Compared with single-objective solutions (Table C1), both multi-objective outcomes exhibited intermediate latitudinal variability: their coefficients of variation fell between highly heterogeneous profiles such as water provision (CV = 0.816) and more even profiles such as carbon storage (CV = 0.582). These spatial patterns and latitudinal reassignments were associated with corresponding differences in objective-level performance, summarized in Fig. 4.

### 3.3. Trade-offs among objectives in multi-objective solutions

Overall, the results show that multi-objective solutions occupied intermediate positions in objective space, balancing asymmetric trade-offs among criteria rather than privileging any single objective. Figure 4 summarizes the trade-offs among criteria for the F-ex and F-in scenarios, expressed relative to the corresponding single-objective optima. In both panels, single-objective solutions defined extreme points of objective space (edges), reaching 100% performance on their own axis while exhibiting reduced performance on the remaining criteria. The multi-objective solution (purple polygon) occupied an intermediate position in objective space, representing a compromise that balanced gains across criteria rather than maximizing any single objective in isolation.

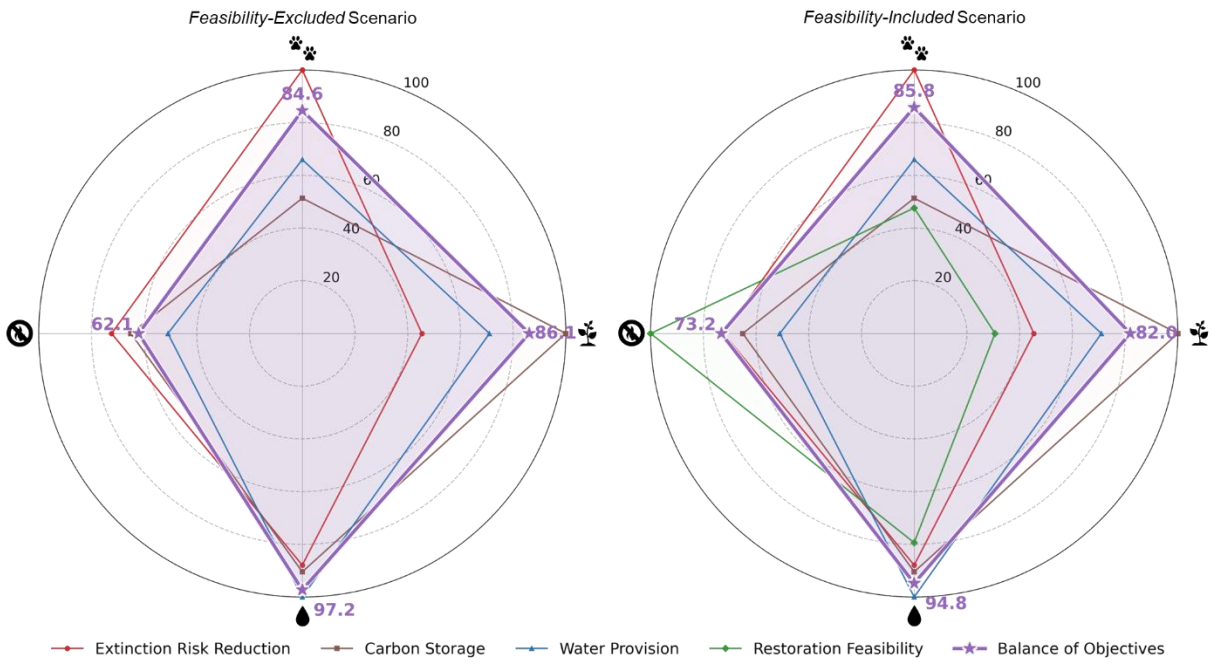


**Fig. 4 | Trade-offs among criteria in multi-objective scenarios excluding (F-ex, left) and including (F-in, right) restoration feasibility.** Radar charts show the performance of single-objective and multi-objective solutions relative to their corresponding single-objective optima (represented by the 100). Single-objective solutions achieve 100% for their optimized criterion and exhibit lower performance on the remaining axes. The purple polygon represents the multi-objective compromise solution in each scenario, with purple labels reporting its performance scores across criteria. In the feasibility-excluded scenario, the restoration feasibility single-objective profile is omitted from the chart, although the axis is maintained for comparative purposes.

Based on Table C2, single-objective solutions exhibited pronounced asymmetries in objective-level performance across criteria. These asymmetries were directional rather than even: optimizing carbon storage maintained a high proportion of water provision (90.4%), whereas optimizing water provision led to lower performance in carbon storage (71.0%), indicating non-reciprocal compatibility between objectives.

When aggregated across non-target objectives, these patterns translated into variation in cross-solution performance among single-objective solutions (Table C2). Although each solution achieved its maximum value for the optimized criterion, average performance across remaining objectives differed among criteria. In particular, water provision achieved comparatively high performance across non-target objectives, whereas carbon storage exhibited lower average cross-objective performance. These contrasts highlight asymmetric and non-reciprocal patterns under single-objective optimizations.

In the feasibility-excluded scenario (Fig. 4, left), the multi-objective solution achieved high and relatively uniform performance across the three ecological objectives (Table C2), while feasibility remained comparatively low when not explicitly optimized. Under the feasibility-included formulation (Fig. 4, right; Table C2), feasibility performance increased markedly, while remaining objectives maintained comparably high values.

Overall, both multi-objective solutions achieved higher average performance across objectives than any single-objective solution (cross-objective performance = 82.5% for BO F-ex and 83.9% for BO F-in; Table C2). Although including restoration feasibility introduced trade-offs with other criteria, the resulting gains in feasibility (+11.1 percentage points) and extinction risk reduction (+1.2) exceeded the moderate losses observed for carbon storage (−4.1) and water provision (−2.4). Notably, the concurrent improvement in feasibility and extinction risk reduction indicates a spatial synergy: prioritizing areas with higher likelihood of restoration success also targets locations associated with higher biodiversity value. Consequently, including restoration feasibility improved the overall balance of performance across objectives without inducing substantial reductions in ecological outcomes.

### 3.4. Selection frequency of planning units across the optimization framework

Overall, selection frequency patterns show that the multi-objective F-in solution was primarily supported by units that contributed consistently across objectives, rather than by units uniquely associated with a single criterion. Figure 5 shows the spatial distribution of the selection frequency of units in the F-in solution, summarizing how often each unit was selected across the optimization framework. Selection frequency, computed as the number of optimization runs in which a unit is selected (see **Section 2.6**), serves as a proxy for irreplaceability: higher frequencies correspond to units that consistently contribute across objectives (i.e., are less substitutable), whereas lower values correspond to units whose inclusion depends more directly on a specific objective.

Across the three regions shown in Fig. 5, units with intermediate irreplaceability dominated the solution. In the extreme north (Arica y Parinacota Region), units selected three times represented 48.0% of all selected units, followed by units selected twice (40.1%) and four times (11.9%), and none were selected only once or in all five cases. A similar pattern emerged in central Chile (Santiago Metropolitan Region), where frequency-three units represented 60.6% of the total, followed by frequency-two (35.4%) and frequency-four units (3.8%), while units selected once and five times were negligible (<0.2%). In the extreme south (Magallanes y Antártica Chilena Region), units selected three times also dominated (51.0%), but with a comparatively larger contribution of frequency-four units (26.2%) and a smaller share of frequency-two units (22.5%); units selected once or five times together accounted for less than 0.4% of the total. Despite regional differences in the total number of selected units, these patterns were consistent across regions.

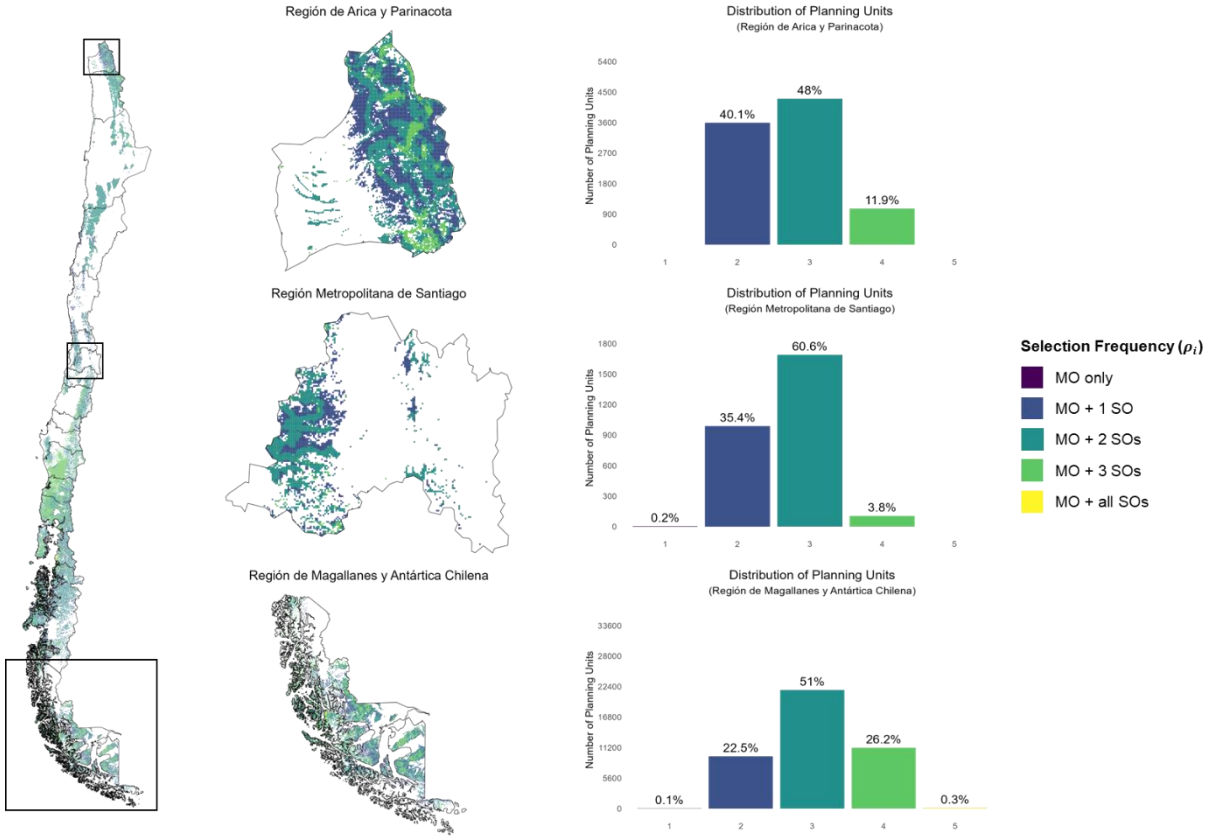


**Fig. 5 | Distribution of selection frequency of planning units across the optimization framework.** Maps show the selection frequency ($\rho_i$) of planning units across continental Chile, with expanded views detailing representative northern (Arica y Parinacota Region), central (Santiago Metropolitan Region), and southern (Magallanes y Antártica Chilena Region) regions. Values on the scale range from 1 to 5, indicating how consistently a unit is prioritized. A value of 1 corresponds to units selected exclusively in the multi-objective F-in solution (MO only), while values 2 through 5 correspond to units additionally selected in one to four single-objective solutions (MO + 1–4 SOs). Bar plots summarize the absolute number and proportional distribution of these frequencies within each focal region; missing bars or labels denote zero or negligible proportions.

At the national scale, Fig. C1 confirms these regional patterns. Units selected an intermediate number of times dominated the F-in solution, whereas units selected only once or in all optimization steps remained negligible. This distribution indicates that irreplaceability in the multi-objective solution was primarily associated with units that were consistently—but not universally—selected, rather than with units tied to a single optimization run. Together, Fig. 5 and Fig. C1 indicate that the F-in solution was dominated by units with intermediate to high selection frequencies—reflecting consistent contributions across optimization runs—, and was complemented by a smaller set of units whose selection varied across objectives.

### 3.5. Functional roles of planning units within the multi-objective solution

Overall, the classification of functional roles shows that the F-in compromise solution was dominated by multipurpose units, with objective-specific and balance-supporting units playing secondary but spatially

meaningful functions. Building on the selection-frequency patterns described above, Fig. 6 classifies units into functional categories reflecting how irreplaceability varies across objectives. Units consistently selected across multiple single-objective problems represent highly irreplaceable, multipurpose components of the solution, whereas units selected under more limited objective combinations correspond to more specialized contributions.

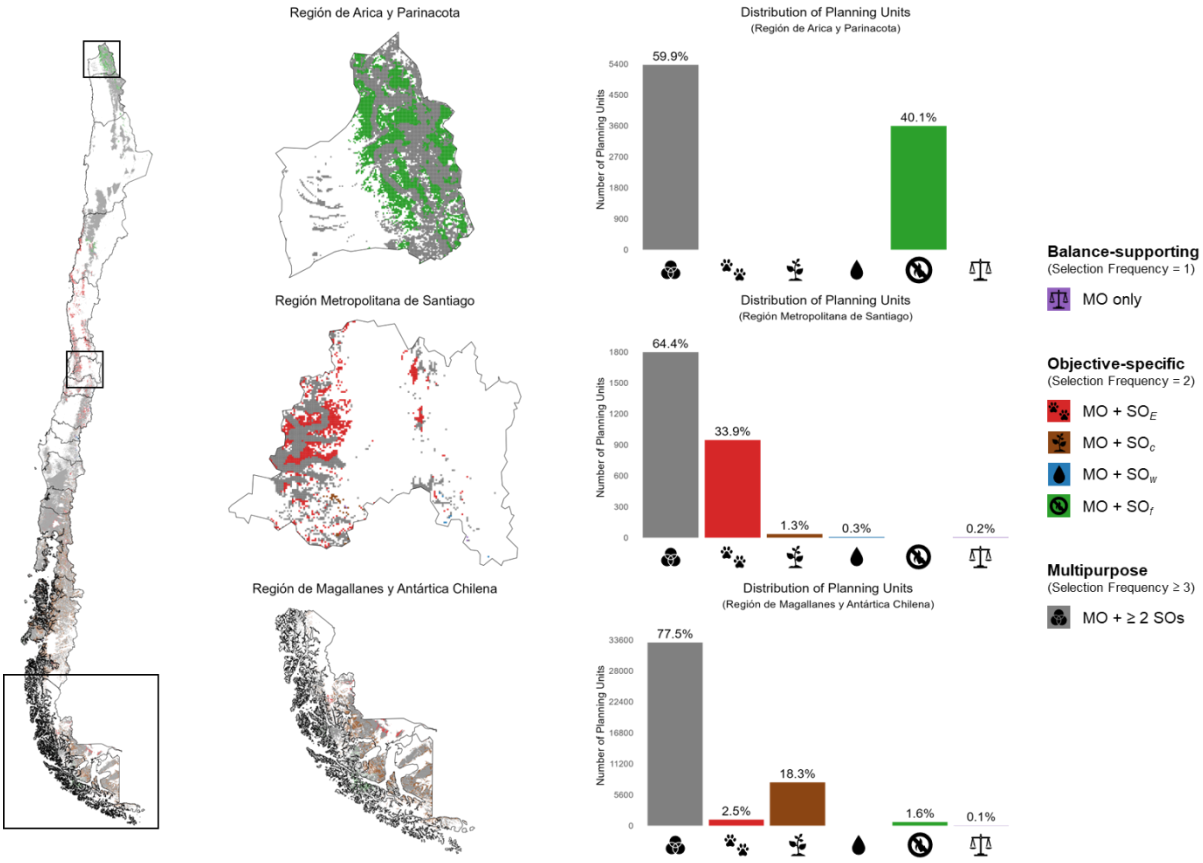


**Fig. 6 | Distribution of functional roles of planning units in the multi-objective solution.** Units are classified into three functional roles based on their selection frequency ($\rho_i$) across the multi-objective (MO) and single-objective (SO) optimization runs. Multipurpose units correspond to those selected in the MO solution and two or more SO runs (MO + ≥ 2 SOs). *Objective-specific* units are selected in the MO solution and exactly one SO run (MO + 1 SO), further distinguished by their specific target: extinction risk reduction (SO$_E$), carbon storage (SO$_c$), water provision (SO$_w$), or restoration feasibility (SO$_f$). *Balance-supporting* units are selected exclusively in the MO solution (MO only). Maps show the spatial distribution of these roles across representative northern (Arica y Parinacota Region), central (Santiago Metropolitan Region), and southern (Magallanes y Antártica Chilena Region) regions of Chile. Bar plots summarize the absolute number and relative proportion of units assigned to each role within these regions; missing bars or labels denote zero or negligible proportions.

Across all regions shown in Fig. 6, multipurpose units constituted the largest fraction of the solution. In the Arica y Parinacota Region, they represented 59.9% of selected units, while the remaining 40.1% corresponded exclusively to restoration feasibility–specific units; no units were classified as objective-specific for extinction risk reduction, carbon storage, or water provision. In the Santiago Metropolitan Region, multipurpose units

constituted 64.4% of the solution, followed by extinction risk reduction–specific units (33.9%), while all remaining functional categories each contributed less than 2%. In the Magallanes y Antártica Chilena Region, multipurpose units accounted for 77.5% of selected units, while carbon storage–specific units comprised 18.3%; each remaining role contributed less than 3%.

At the national scale, Fig. C2 confirms the predominance of multipurpose units. Overall, 80.1% of all selected units fell into this category, indicating that selection frequency in the F-in solution was largely associated with consistent contributions across multiple objectives. Objective-specific units formed a smaller fraction, with carbon storage–specific units accounting for 11.7%, extinction risk reduction–specific units for 5.32%, and restoration feasibility–specific units for 2.56%. Balance-supporting units—selected only in the multi-objective optimization—and water provision–specific units were rare, together representing less than 0.4% of all selected units.

Together, Figures 5, 6, and C2 demonstrate that irreplaceability in the F-in solution was primarily supported by a broad backbone of multipurpose units, complemented by a smaller, spatially heterogeneous set of objective-specific units. Balance-supporting units contributed marginally, indicating that spatial allocation was predominantly associated with units consistently valuable across objectives rather than with units emerging exclusively from the compromise framework.

## 4. Discussion

This study contributes to spatial restoration planning by operationalizing ecological restoration feasibility as an explicit objective within a multi-objective optimization framework. By employing a goal programming approach, we provide a structured method to reconcile competing ecological objectives, minimizing deviations from single-objective aspiration levels to identify balanced compromise solutions. Unlike traditional spatial planning approaches, our formulation incorporates feasibility directly into the objective space. This ensures that its influence on spatial priorities and trade-offs is evaluated in an analytically consistent and interpretable way.

Because the feasible region (Φ) and optimization structure were held constant across scenarios, the observed differences among solutions can be entirely linked to objective interactions. This controlled assessment reveals that incorporating feasibility (F-in) significantly reshapes spatial priorities and the internal configuration of restoration solutions, while inducing only moderate changes in overall ecological performance relative to the feasibility-excluded scenario. Our spatial diagnostics, based on selection frequency, further indicate that these changes are systematic, reflecting a deliberate rebalancing toward areas with higher expected persistence without compromising core biodiversity or ecosystem service outcomes.

While a growing body of literature integrates biodiversity and ecosystem services into multi-objective planning (e.g., Strassburg et al., 2018, 2020; Sala et al., 2021; Schüler & Bustamante, 2022; Srivathsa et al., 2023; Deléglise et al., 2024; Gopalakrishna et al., 2024; B. A. Williams et al., 2024; Drever et al., 2025), restoration feasibility has typically been treated either as a hard constraint (locked-out) or as a *post hoc* screening filter (Orsi & Geneletti, 2010; Zamorano-Elgueta et al., 2025). Our results reframe this conventional approach by

demonstrating that feasibility is not merely a constraint but a structuring dimension of restoration planning. By optimizing feasibility alongside ecological targets, we move beyond viewing feasibility as a hurdle and instead position it as a driver of spatial allocation, offering a more robust and policy-relevant framework for achieving large-scale restoration commitments such as Target 2 of the Kunming–Montreal Global Biodiversity Framework.

### 4.1. A structured optimization framework as a basis for interpretable restoration planning

From a methodological perspective, the framework highlights several advantages of exact multi-objective optimization for large-scale restoration planning, particularly through the combination of controlled experimental design, explicit benchmark solutions, and complementary spatial diagnostics. By relying on exact optimization, the approach delivers solutions whose performance and trade-offs can be evaluated relative to explicit constraints and benchmarks, with solution quality assessed using the optimality gap (MIP gap; see **Section 3**, *Experimental setting*). This contrasts with heuristic approaches, which are computationally more efficient but provide limited guarantees regarding solution quality and the magnitude of trade-off among objectives (Beyer et al., 2016; Schuster et al., 2020). At the same time, the computational results indicate that the proposed MILP framework remains tractable at the national scale, consistently achieving high-quality solutions with negligible optimality gaps, which supports its practical applicability for large-scale restoration planning despite the inherent complexity of the problem.

Equally important, the interpretability of the framework emerges not only from the use of exact optimization, but also from its controlled experimental design and the integration of complementary diagnostics applied to a consistent set of optimization outputs. By ensuring that all optimization runs share an identical feasible region, constraint structure, and decision space, the framework enables meaningful comparisons across single-objective and multi-objective solutions, isolating the effect of each objective on spatial allocation and performance trade-offs.

Within this structure, interpretability is achieved through the joint use of single-objective benchmarks, compromise solutions, and selection-frequency diagnostics derived from the same optimization ensemble. This combination allows the final solution to be unpacked in terms of its structural components. Rather than considering the compromise as a black box, the framework clarifies *why* specific units are selected and *how* their roles differ within the broader solution.

The explicit use of single-objective optimizations is therefore not merely a computational device, but a core design feature that enables interpretability and functional decomposition of solutions. These reference solutions contextualize trade-offs, support the identification of synergies, and enable the functional classification of units. Such transparency is particularly relevant for decision-support applications, where explainability and reproducibility are often as important as numerical optimality. Against this methodological backdrop, the results provide insight into how explicitly optimizing feasibility reshapes the spatial structure and performance of restoration solutions.

### 4.2. Feasibility as a restructuring dimension in multi-objective restoration planning

Viewed through this framework, single-objective optimizations reveal differentiated spatial patterns along the latitudinal gradient, reflecting the distinct spatial signatures associated with each criterion. Such contrasts are consistent with previous studies showing that solutions obtained under different objectives tend to concentrate in different regions due to their underlying ecological and socio-economic drivers (Schüler & Bustamante, 2022; Gopalakrishna et al., 2024; B. A. Williams et al., 2024). These contrasting patterns provide a baseline for evaluating multi-objective solutions. When objectives are combined, compromise solutions exhibit intermediate variability in both spatial distribution and performance, consistent with the integration of heterogeneous priorities rather than convergence toward a single-objective extreme.

Including restoration feasibility modifies the multi-objective solution through spatial substitutions under fixed area constraints, broadening latitudinal coverage and rebalancing objective performance while preserving the total restored area (Fig. 3). The feasibility-included formulation introduces new trade-offs among objectives; however, gains achieved in restoration feasibility and extinction risk reduction exceed the moderate losses observed for carbon storage and water provision. Importantly, this pattern reflects a spatial synergy: prioritizing areas with higher likelihood of restoration success also tends to capture habitats of high importance for threatened species. Thus, planning for feasibility does not merely redistribute benefits across objectives, but can actively enhance biodiversity outcomes. As a result, incorporating restoration feasibility yields a net improvement in overall performance under the equal-weight normalized aggregation used for comparison with the feasibility-excluded solution (Fig. 4; Table C2).

In this sense, feasibility primarily acts as a re-allocation driver, reshaping spatial priorities within a constant budget without reducing the total ecological performance achieved. This distinction is particularly relevant for prioritization initiatives in which feasibility is commonly treated as an external filter. Our results suggest that explicitly optimizing feasibility integrates ecological trade-offs into the decision process, enabling spatial reconfiguration with limited ecological losses and reinforcing feasibility as a core planning dimension rather than a screening criterion. These spatial substitutions are accompanied by corresponding changes in objective-level performance, which helps clarify the trade-offs introduced by explicitly incorporating feasibility.

### 4.3. Asymmetric trade-offs and cross-performance of multi-objective solutions

At the level of objective space, these patterns further highlight the advantages of the multi-objective approaches. Single-objective solutions occupy the extreme points of objective space, achieving maximal performance for the targeted criterion while exhibiting heterogeneous performance across non-target objectives (Fig. 4; Table C2). Comparable asymmetric trade-off profiles have been reported, reflecting differences in the spatial overlap among objectives (Strassburg et al., 2018; Sala et al., 2021; Drever et al., 2025). In our case, these asymmetries stem not only from spatial overlap among ecological objectives, but also from the inclusion of feasibility as a competing criterion in the optimization process. When contrasted with single-objective benchmarks, the

resulting multi-objective solutions occupy intermediate positions in objective space, representing balanced compromises across criteria.

Cross-solution performance metrics reveal marked asymmetries among single-objective solutions. Although each solution reaches its maximum value for the optimized criterion, performance across remaining objectives varies. These patterns show that objectives differ not only in their spatial expression, but also in their degree of structural compatibility with other criteria. This compatibility is not symmetric: optimizing one objective may preserve a considerable share of performance in others, but the converse does not necessarily hold. As a result, some objectives act as integrators, maintaining high performance across multiple criteria when optimized, whereas others are more specialized and lead to larger losses in non-target objectives under single-objective optimization. Carbon storage illustrates this specialized behavior, as its concentrated spatial pattern is associated with lower cross-solution performance, reflecting limited compatibility with other objectives when optimized in isolation.

Both multi-objective solutions achieve higher average cross-objective performance than any single-objective alternative. The feasibility-included solution entails moderate reductions in some ecological objectives, but gains in restoration feasibility and extinction risk reduction outweigh these losses, resulting in higher overall performance across the system. In this sense, multi-objective optimization balances objectives with limited reciprocal compensation, mitigating asymmetries in objective-level performance. These results suggest that compromise solutions are not merely intermediate outcomes, but can outperform collections of single-objective strategies from a system-wide perspective that considers joint performance across all objectives, while making trade-offs explicit and quantifiable. However, aggregate performance alone does not reveal how these trade-offs are internally accommodated within the spatial solution.

### 4.4. Structural synergies and functional roles in the compromise solution

To move beyond aggregate performance, analysis of selection frequency provides insight into the internal configuration of the compromise solution. Units consistently selected across objectives form a broad backbone of relatively irreplaceable, multipurpose areas that underpin the solution at both regional and national scales (Figs. 5–6). Similar backbone patterns have been observed, with areas contributing to multiple ecological features tending to emerge (Sala et al., 2021; Schüler & Bustamante, 2022; Eckert et al., 2023; Gopalakrishna et al., 2024). The persistence of these backbones across F-ex and F-in scenarios indicates that feasibility optimization reorganizes the composition of compromise solutions without breaking their core spatial support. These units represent locations where multiple objectives coincide spatially, revealing synergies that emerge from the spatial co-occurrence of ecological characteristics and feasibility conditions, rather than being imposed *a priori* by the optimization formulation. These spatial patterns represent the geographic expression of the differentiated functional roles observed in objective space.

Notably, units with the highest irreplaceability (i.e., those with the highest selection frequency across objectives) constitute only a limited fraction of the selected areas. The internal configuration of the solution is

instead dominated by units with intermediate selection frequencies, which play a key role in accommodating spatially localized trade-offs where objectives partially align. Objective-specific units, although less frequent, contribute by resolving tensions among criteria in areas of lower structural compatibility, supporting balanced performance across objectives. Units selected exclusively under the multi-objective formulation remain comparatively rare, indicating that the compromise solution is largely anchored in areas that already contribute under single-objective formulations, rather than resulting from entirely novel selections.

In northern and central Chile, structural synergies typically involve the contribution of two objectives, whereas in southern regions they often extend to three objectives (Fig. 6). The persistence of these patterns at the national scale (Figs. C1–C2) suggests that complementarities among objectives are rooted in underlying ecological and landscape characteristics, rather than being artifacts of the optimization algorithm or the spatial distribution of restoration actions per se. This decomposition clarifies how trade-offs in objective space translate into differentiated functional roles in geographic space, enhancing the interpretability of the multi-objective solution. These differentiated functional roles also help explain why the resulting spatial priorities remain ecologically coherent when interpreted against the broader ecosystem context of Chile.

### 4.5. Ecological interpretation of spatial restoration priorities

Consistent with this internal structure, the multi-objective solutions also exhibit ecologically coherent spatial patterns when examined in relation to the distribution and conservation status of terrestrial ecosystems in Chile. Although biodiversity conservation in the model is explicitly represented through species-level extinction risk reduction, both compromise solutions show substantial spatial overlap with ecosystems classified as Critically Endangered (CR) or Endangered (EN). Approximately 48.6% of the area selected under the feasibility-excluded solution (F-ex) and 42.7% under the feasibility-included solution (F-in) overlap with ecosystems belonging to these categories (Pliscoff et al., 2025).

Importantly, ecosystem threat status is not explicitly optimized in the model, making this overlap an emergent property of the spatial prioritization rather than a built-in outcome. The observed convergence suggests that areas contributing strongly to species-level extinction risk reduction also tend to coincide spatially with ecosystems that have undergone long-standing and intense degradation processes. This pattern can be explained by the fact that highly threatened species are often confined to remaining, less-disturbed refugia, which tend to score higher under our feasibility proxies. In this sense, planning for feasibility not only avoids heavily degraded areas, but can also direct restoration efforts toward locations that are both more viable and more relevant for biodiversity conservation. This reinforces the ecological coherence of the solutions beyond their formulation in objective space.

The terrestrial ecosystems most frequently represented in both solutions correspond primarily to deciduous and sclerophyllous forests in central–southern Chile, temperate and temperate–cold Andean forests, and Mediterranean and high-Andean shrublands in northern and central regions. These ecosystem types refer to the underlying potential or reference ecosystems associated with the selected planning units, rather than their

current land cover, which consists of degraded or transformed conditions (e.g., croplands, plantations, or grasslands) identified as suitable for restoration. This distribution is consistent with the historical concentration of land-use change, habitat fragmentation, recurrent fires, and extractive pressures affecting Chilean landscapes, which have jointly driven ecosystem degradation and biodiversity loss over large spatial extents (Echeverría et al., 2006; Schulz et al., 2010; Miranda et al., 2015; Garreaud et al., 2019; Smith-Ramírez et al., 2021; Orrego et al., 2023).

Comparison between F-ex and F-in indicates that explicitly including restoration feasibility induces a moderate redistribution of restoration effort among ecosystem types, without materially shifting the concentration of biodiversity-related benefits within highly degraded landscapes. In both scenarios, restoration priorities remain largely anchored in ecosystems facing high conservation concern, while feasibility acts to reshuffle spatial allocation within this set rather than displacing priorities toward ecologically marginal systems.

From a modelling perspective, these patterns indicate that restoration feasibility operates primarily as a spatial reallocation mechanism rather than as a driver of ecological exclusion. Explicitly optimizing feasibility reshapes where restoration actions are allocated within the landscape, while preserving the underlying ecological signal associated with biodiversity conservation. This ecological coherence strengthens the relevance of the framework not only as an analytical tool, but also as a robust foundation for restoration policy and management.

### 4.6. Policy and management implications for restoration decision-making

Building on this ecological coherence and the explicit representation of trade-offs within the optimization framework, several implications emerge for policy and restoration decision-making. First, the finding that feasibility can be incorporated without substantial degradation of ecological performance supports its integration early in the planning process. This is particularly relevant for national-scale initiatives linked to global commitments such as Target 2 of the Kunming–Montreal Global Biodiversity Framework, where restoration success depends on aligning ecological priorities with implementation constraints (CBD, 2022; FAO et al., 2024), and feasibility considerations may ultimately determine whether restoration efforts are achievable in practice. In this context, explicitly optimizing feasibility helps ensure that area-based targets translate into effective restoration and long-term ecological integrity (*sensu* Target 2), providing a concrete operational pathway to reduce the risk of costly, avoidable restoration failures on the ground.

At the same time, the results highlight an important limitation inherent to how feasibility is operationalized. By representing feasibility as a composite index based on exposure to recurrent ecological threats, maximizing feasibility corresponds to a deliberately risk-averse strategy that prioritizes areas with higher expected persistence by avoiding high-risk conditions. This operationalization provides a conservative baseline for persistence-oriented restoration planning, consistent with approaches that rely on avoidance-based proxies, such as distance from human pressures and land-use conflict indicators (e.g., Orsi & Geneletti, 2010; Zamorano-Elgueta et al., 2025). In this sense, the feasibility-included solution can be interpreted as a conservative, persistence-oriented restoration portfolio suited to large-scale implementation contexts characterized by limited

capacity for intensive post-restoration management, as often associated with Target 2 commitments, prioritizing long-term viability under limited risk tolerance.

Consistent with this perspective, our framework conceptualizes restoration primarily as a large-scale process of assisted ecological recovery, in which natural regeneration is facilitated through targeted, low-intensity interventions. By prioritizing landscapes where key constraints are lower, the model assumes that reducing environmental pressures, together with enabling conditions for regeneration, is a primary driver of sustained ecosystem recovery at the national scale. This reflects the practical reality that intensive, site-specific interventions are often unfeasible across millions of hectares, while assisted natural regeneration offers a scalable pathway for restoration under such conditions.

However, our findings point to limited spatial overlap between areas of high ecological feasibility and those providing substantial biodiversity and ecosystem service co-benefits, while also suggesting that low-risk landscapes are scarce. As a consequence, feasibility shows the lowest cross-objective performance under single-objective optimization and remains the weakest compensating objective within the multi-objective solution (Fig. 4; Table C2). Achieving higher levels of feasibility would therefore require going beyond spatial avoidance toward threat-management strategies, such as fire prevention and invasive species control, as well as institutional and governance interventions aimed at reducing underlying drivers of degradation (e.g., land-use regulation, enforcement, or incentive schemes). These strategies are inherently more complex to represent, implement, and finance—particularly at large spatial scales—yet may be essential for achieving long-term restoration outcomes in high-risk landscapes.

Second, the dominance of multipurpose units suggests that coordinated restoration actions can deliver multiple benefits simultaneously, reducing the need for fragmented or highly objective-specific interventions (Fig. 6). Nonetheless, regional variation in functional roles indicates that contributions to national restoration objectives are spatially differentiated, with implications for budget allocation, inter-regional coordination, and the design of complementary regional strategies. Importantly, these spatial differences reflect underlying biogeographic variation across the study area, suggesting that restoration planning and prioritization may benefit from being structured around biogeographic zones rather than solely administrative regions. In this context, biogeographic units can provide a more ecologically coherent basis for decision-making, particularly in countries such as Chile where strong latitudinal gradients and ecosystem contrasts shape restoration opportunities and constraints, including macro-regional or cross-border planning contexts.

Finally, by quantifying trade-offs and cross-objective performance, the framework provides a transparent basis for negotiation among stakeholders. Decision-makers can evaluate how alternative priorities influence both spatial allocation and overall outcomes, supporting more defensible and evidence-based restoration strategies. In particular, the framework makes visible the opportunity costs associated with single-objective or narrowly focused strategies by revealing broader losses in non-target objectives that would otherwise remain implicit in restoration planning. In this sense, the framework is suitable for iterative and interactive decision-making processes, in which priorities, weights, and constraints can be explored jointly with decision-makers, while

maintaining a transparent and formally defined optimization framework. This transparency supports more efficient and balanced use of limited restoration resources, strengthening the link between scientific evidence and policy decision-making. At the same time, translating these insights into practice requires acknowledging the assumptions and limitations that accompany large-scale optimization frameworks.

### 4.7. Generalizability, limitations, and future directions

Despite its generality and policy relevance, the framework remains subject to several limitations that also point to productive directions for future research. Although applied here to continental Chile, the proposed framework is transferable to other geographic contexts and planning problems, as its feasibility component can be re-parameterized using region-specific disturbance regimes (e.g., drought, flooding, grazing pressure) without modifying the underlying optimization structure. While the objectives optimized here reflect criteria with broad relevance across terrestrial, freshwater, and marine–coastal environments, the framework remains flexible and can be extended to alternative objectives, constraints, and spatial resolutions.

As with most large-scale planning exercises, the framework reflects an inherent trade-off between spatial resolution and computational and data efficiency. While large-scale analyses necessarily rely on lower-resolution representations that promote coordination, cooperation, and economies of scale, finer-resolution, local-scale planning can capture higher ecological and socio-environmental detail but is often constrained by data availability and limited scalability.

More broadly, the present formulation relies on deterministic inputs and assumes that all spatial data layers are known with certainty. In practice, however, ecological and socio-environmental data are often scarce, incomplete, or uneven in quality at national scales, which may affect both the accuracy of parameter estimates and the robustness of spatial prioritization outcomes. These limitations are particularly relevant in data-limited contexts, where uncertainty in species distributions, ecosystem services, or disturbance proxies may propagate through the optimization process.

In addition, the computational complexity of solving large-scale mixed-integer linear programs can pose practical constraints, especially when extending the framework to higher spatial resolutions, additional objectives, or more complex constraint structures. Although the present implementation remains tractable at the national scale, future applications may require decomposition strategies, heuristic approximations, or parallel computing approaches to ensure scalability.

Model outcomes are also sensitive to parameter choices embedded in the formulation, particularly regarding how restoration feasibility is operationalized. The feasibility index is constructed as a parsimonious, additive combination of standardized proxies, assigning equal weight to disturbances (fire frequency, anthropogenic pressure, and invasive species richness). Although this enhances transparency, alternative weighting or aggregation schemes could modify feasibility rankings and spatial allocation outcomes. However, our choice to assign equal importance to all feasibility dimensions provides a transparent and parsimonious baseline. This avoids the introduction of subjective weights that could bias prioritization outcomes, a critical consideration for

ensuring that planning frameworks remain defensible and reproducible in policy-making contexts. Under this premise, the aim of this study is not to propose a definitive feasibility map, but to demonstrate how a persistence-oriented feasibility representation can be explicitly embedded within a multi-objective MILP-based SCP framework. The framework is therefore designed to accommodate alternative feasibility formulations rather than prescribe a single one.

Similarly, at the optimization level, objective performances were normalized and aggregated using equal weights. While this neutral baseline facilitates transparent comparison across objectives, it does not necessarily reflect context-specific preferences. Future applications could explore alternative weighting schemes informed by expert elicitation, stakeholder input, or policy priorities. In this study, goal programming was deliberately employed as a synthesis tool to generate a single, interpretable compromise solution relative to single-objective benchmarks, rather than to perform an exhaustive mapping of the Pareto frontier. This choice reflects our core focus on linking trade-offs in objective space to the spatial configuration and functional roles of planning units. However, alternative Pareto-oriented MILP formulations (such as ε-constraint or reference-point methods) could be used in future applications to explore the efficient frontier more comprehensively, particularly where the explicit characterization of all trade-offs is required.

Feasibility was operationalized through a deliberately risk-averse approach that prioritizes areas with lower exposure to threats. While effective for identifying feasible locations, this approach does not guarantee meaningful ecological gains, particularly in degraded but high-risk systems where restoration may be feasible but of limited ecological relevance. Future extensions could incorporate threat-management objectives as well as restoration-need targets—based on native habitat losses, changes in vegetation productivity, or ecological risk assessments—to better align feasibility with potential ecological benefits.

Additional limitations relate to implementation dynamics. Feasibility was represented as a static spatial layer, whereas it is likely to evolve over time in response to policies, socio-economic changes, or management interventions. The analysis further focuses on a fixed area budget and does not explore alternative budget levels, phased implementation pathways, or dynamic or stochastic extensions that could better represent temporal change and uncertainty.

Overall, these considerations outline directions for further research, including alternative objective formulations, multi-scale architectures, and dynamic feasibility models. Ultimately, by operationalizing biodiversity conservation, ecosystem services, and restoration feasibility within a unified optimization framework, our approach provides a generalizable, scalable, and transferable method for large-scale spatial restoration planning. Its application to Chile illustrates how limited resources can be allocated efficiently, how trade-offs among objectives can be quantified, and how balanced spatial solutions can be structured while explicitly linking spatial prioritization to the likelihood of long-term restoration success. Beyond this specific application, the framework can support the design of robust restoration strategies that align ambitious global policy commitments with implementable and persistent ecological outcomes.

**Acknowledgments**

M.M.-F. was supported by the National Research and Development Agency of Chile (ANID) through a doctoral scholarship (No. 72220359) and FONDECYT Grant No. 1220830, and by the European Union's Horizon 2020 research and innovation programme under the Marie Skłodowska-Curie RISE Grant Agreement No. 101007950 (DecisionES). M.J.M.-H. was supported by ANID Millennium Science Initiative Programme – Code ICN2019_015 and ANID FONDECYT ANILLO ACT240004. B.L.-B. was supported by ANID Millennium Science Initiative Programme – Code ICN2019_015, ANID FONDECYT ANILLO ACT240004, and the European Union's Horizon 2020 research and innovation programme under the Marie Skłodowska-Curie RISE Grant Agreement No. 101007950 (DecisionES). P.P. was supported by FONDECYT Grant No. 1261139. M.J.M.-H., E.A.-M., B.L.-B., M.P.-B., E.F.-L., P.P., C.S.-R., and A.P. were supported by ANID/BASAL FB210006.

## References

Abarca, H., Morán-Ordoñez, A., Villero, D., Guinart, D., Brotons, L., & Hermoso, V. (2022). Spatial prioritisation of management zones in protected areas for the integration of multiple objectives. Biodiversity and Conservation, 31(4), 1197-1215. https://doi.org/10.1007/s10531-022-02383-z

Alagador, D., & Cerdeira, J. O. (2022). Operations research applicability in spatial conservation planning. Journal of Environmental Management, 315, 115172. https://doi.org/10.1016/j.jenvman.2022.115172

Altamirano A, Salas C, Yaitul V, Smith-Ramírez C, Ávila A (2013) Influencia de la heterogeneidad del paisaje en la ocurrencia de incendios forestales en Chile Central. *Revista de Geografía Norte Grande* 55:157–170

Álvarez-Miranda, E., Salgado-Rojas, J., Hermoso, V., Garcia-Gonzalo, J., & Weintraub, A. (2020). An integer programming method for the design of multi-criteria multi-action conservation plans. Omega, 92, 102147. https://doi.org/10.1016/j.omega.2019.102147

Aronson J, Blignaut JN, Milton SJ (2011) Restoring natural capital: science, business, and practice. Island Press, Washington D.C.

Bayer, A. D., Lautenbach, S., & Arneth, A. (2023). Benefits and trade-offs of optimizing global land use for food, water, and carbon. Proceedings of the National Academy of Sciences, 120(42), e2220371120. https://doi.org/10.1073/pnas.2220371120

Beyer, H. L., Dujardin, Y., Watts, M. E., & Possingham, H. P. (2016). Solving conservation planning problems with integer linear programming. Ecological Modelling, 328, 14-22. https://doi.org/10.1016/j.ecolmodel.2016.02.005

Billionnet, A. (2013). Mathematical optimization ideas for biodiversity conservation. European Journal of Operational Research, 231(3), 514-534. https://doi.org/10.1016/j.ejor.2013.03.025

Bonn Challenge (2024) About the challenge. Retrieved from https://www.bonnchallenge.org

Bottrill MC, Joseph LN, Carwardine J, Bode M, Cook C, Game ET, Grantham H, Kark S, Linke S, McDonald-Madden E, Pressey RL, Walker S, Wilson KA, Possingham HP (2008) Is conservation triage just smart decision making? *Trends in Ecology & Evolution* 23(12):649–654

Carroll, C., Hoban, S., & Ray, J. C. (2024). Lessons from COP15 on effective scientific engagement in biodiversity policy processes. Conservation Biology, 38, e14192. https://doi.org/10.1111/cobi.14192

Castillo-Mandujano J, Smith-Ramírez C (2022) The need for holistic approach in the identification of priority areas to restore: a review. *Restoration Ecology* e13637

CBD (Convention on Biological Diversity) (2022) Kunming-Montreal Global Biodiversity Framework. Retrieved from https://www.cbd.int

Cheng, H.-C., Château, P.-A., & Chang, Y.-C. (2015). Spatial zoning design for marine protected areas through multi-objective decision-making. Ocean & Coastal Management, 108, 158-165. https://doi.org/10.1016/j.ocecoaman.2014.08.018

Cho, S., Mingie, J. C., Kang, N., Zhu, G., & Upendram, S. (2023). Understanding the differences between single- and multiobjective optimization for the conservation of multiple species. Natural Resource Modeling, 36(1), e12356. https://doi.org/10.1111/nrm.12356

Cho, S.-H., & Sharma, B. P. (2020). Optimal spatial budget distribution of forest carbon payments that balances the returns and risks associated with conservation costs. Environment, Development and Sustainability, 22(8), 7239-7267. https://doi.org/10.1007/s10668-019-00486-2

CONAMA (Comisión Nacional de Medio Ambiente) (2006) Estudio de la variabilidad climática en Chile para el siglo XXI. Informe Final. Universidad de Chile, Santiago, Chile

Crossman ND, Bryan BA (2006) Systematic landscape restoration using integer programming. *Biological Conservation* 128(3):369–373

Dai, W., & Ratick, S. J. (2014). Integrating a Raster Geographical Information System with Multi-Objective Land Allocation Optimization for Conservation Reserve Design. Transactions in GIS, 18(6), 936-949. https://doi.org/10.1111/tgis.12085

De Castro-Pardo, M., & Azevedo, J. C. (2021). A Goal Programming Model to Guide Decision-Making Processes towards Conservation Consensuses. Sustainability, 13(4), 1959. https://doi.org/10.3390/su13041959

de Groot, R. S., Alkemade, R., Braat, L., Hein, L., & Willemen, L. (2010). Challenges in integrating the concept of ecosystem services and values in landscape planning, management and decision making. *Ecological Complexity*, *7*(3), 260–272. https://doi.org/10.1016/j.ecocom.2009.10.006

Deléglise, H., Justeau-Allaire, D., Mulligan, M., Espinoza, J. C., Isasi-Catalá, E., Alvarez, C., ... & Palomo, I. (2024). Integrating multi-objective optimization and ecological connectivity to strengthen Peru's protected area system towards the 30* 2030 target. Biological Conservation, 299, 110799.

Di Minin, E., Soutullo, A., Bartesaghi, L., Rios, M., Szephegyi, M. N., & Moilanen, A. (2017). Integrating biodiversity, ecosystem services and socio-economic data to identify priority areas and landowners for conservation actions at the national scale. Biological Conservation, 206, 56-64. https://doi.org/10.1016/j.biocon.2016.11.037

Domisch, S., Kakouei, K., Martínez-López, J., Bagstad, K. J., Magrach, A., Balbi, S., Villa, F., Funk, A., Hein, T., Borgwardt, F., Hermoso, V., Jähnig, S. C., & Langhans, S. D. (2019). Social equity shapes zone-selection: Balancing aquatic biodiversity conservation and ecosystem services delivery in the transboundary Danube River Basin. Science of The Total Environment, 656, 797-807. https://doi.org/10.1016/j.scitotenv.2018.11.348

Drever, C. R., Long, A. M., Cook-Patton, S. C., Celanowicz, E., Fargione, J., Fisher, K., Hounsell, S., Kurz, W. A., Mitchell, M., Robinson, N., Pither, R., Schuster, R., Deziel, V., & Xu, Z. (2025). Restoring forest cover at diverse sites across Canada can balance synergies and trade-offs. One Earth, 8(2), 101177. https://doi.org/10.1016/j.oneear.2025.101177

Duarte CM, Middelburg JJ, Caraco N (2023) Restoration priorities for ecosystems under global change: biodiversity and connectivity considerations. *Global Ecology and Biogeography* 32(3):205–220

Dujardin, Y., & Chadès, I. (2018). Solving multi-objective optimization problems in conservation with the reference point method. PLOS ONE, 13(1), e0190748. https://doi.org/10.1371/journal.pone.0190748

Echeverría C, Coomes DA, Salas J, Rey-Benayas JM, Lara A, Newton A (2006) Rapid deforestation and fragmentation of Chilean temperate forests. *Biological Conservation* 130(4):481–484

Eckert, I., Brown, A., Caron, D., Riva, F., & Pollock, L. J. (2023). 30×30 biodiversity gains rely on national coordination. Nature Communications, 14(1), 7113. https://doi.org/10.1038/s41467-023-42737-x

FAO (Food and Agriculture Organization of the United Nations), ITPS (Intergovernmental Technical Panel on Soils) (2020) Global soil organic carbon map (GSOCmap) v1.5: Technical Report. FAO, Rome

FAO (Food and Agriculture Organization of the United Nations), SCBD (Secretariat of the Convention on Biological Diversity), & SER (Society for Ecological Restoration). (2024). Delivering restoration outcomes for biodiversity and human well-being: Resource guide to Target 2 of the Kunming-Montreal Global Biodiversity Framework. Rome, Montreal, Canada, and Washington, DC. https://doi.org/10.4060/cd2925en

Ferrier, S., Pressey, R. L., & Barrett, T. W. (2000). A new predictor of the irreplaceability of areas for achieving a conservation goal, its application to real-world planning, and a research agenda for further refinement. *Biological Conservation*, 93(3), 303–325.

Fooks, J. R., & Messer, K. D. (2012). Maximizing conservation and in-kind cost share: Applying Goal Programming to forest protection. Journal of Forest Economics, 18(3), 207-217. https://doi.org/10.1016/j.jfe.2012.04.001

Fuentes-Castillo, T., Scherson, R. A., Marquet, P. A., Fajardo, J., Corcoran, D., Román, M. J., & Pliscoff, P. (2019). Modelling the current and future biodiversity distribution in the Chilean Mediterranean hotspot: The role of protected areas network in a warmer future. Diversity and Distributions, 25(12), 1897–1909. https://doi.org/10.1111/ddi.12988

Fuentes-Lillo, E. (2024). Estudio vulnerabilidad terrestre del PNACC BIO: Invasiones biológicas y cambio climático.

Garreaud RD, Boisier JP, Rondanelli R, Montecinos A, Sepúlveda H, Veloso-Aguila D (2019) The Central Chile Mega Drought (2010–2018): a climate dynamics perspective. *International Journal of Climatology* 40(1):421–439

Garreaud, R., Boisier, J. P., Álvarez-Garreton, C., Christie, D. A., Carrasco-Escaff, T., Vergara, I., Chávez, R. O., Aldunce, P., Camus, P., Suazo-Álvarez, M., Masiokas, M., Castro, G., Muñoz, A., Zambrano-Bigiarini, M., Fuster, R., & Godoy, L. (2025). Hyperdroughts in central Chile: Drivers, impacts and projections. Hydrology and Earth System Sciences, 29, 5347–5376. https://doi.org/10.5194/hess-29-5347-2025

GBIF.org (23 July 2024) GBIF occurrence download (Plantae). Retrieved from https://doi.org/10.15468/dl.bxj99t

GBIF.org (29 July 2024) GBIF occurrence download (Animalia). Retrieved from https://doi.org/10.15468/dl.mk7wfj

Geissler, C. H., Haan, N. L., Basso, B., Fowler, A., Landis, D. A., Lark, T. J., & Maravelias, C. T. (2025). A multi-objective optimization model for cropland design considering profit, biodiversity, and ecosystem services. Ecological Modelling, 500, 110954. https://doi.org/10.1016/j.ecolmodel.2024.110954

Giakoumi, S., Richardson, A. J., Doxa, A., Moro, S., Andrello, M., Hanson, J. O., Hermoso, V., Mazor, T., McGowan, J., Kujala, H., Law, E., Álvarez-Romero, J. G., Magris, R. A., Gissi, E., Arafeh-Dalmau, N., Metaxas, A., Virtanen, E. A., Ban, N. C., Runya, R. M., … Katsanevakis, S. (2025). Advances in systematic conservation planning to meet global biodiversity goals. Trends in Ecology & Evolution, 40(4), 395-410. https://doi.org/10.1016/j.tree.2024.12.002

Gopalakrishna, T., Visconti, P., Lomax, G., Boere, E., Malhi, Y., Roy, P. S., Joshi, P. K., Fedele, G., & Yowargana, P. (2024). Optimizing restoration: A holistic spatial approach to deliver Nature's Contributions to People with minimal tradeoffs and maximal equity. Proceedings of the National Academy of Sciences, 121(34), e2402970121. https://doi.org/10.1073/pnas.2402970121

Gurney, G. G., Pressey, R. L., Ban, N. C., Álvarez-Romero, J. G., Jupiter, S., & Adams, V. M. (2015). Efficient and equitable design of marine protected areas in Fiji through inclusion of stakeholder-specific objectives in conservation planning: Social Factors in Conservation Planning. Conservation Biology, 29(5), 1378-1389. https://doi.org/10.1111/cobi.12514

Hanson, J. O., Schuster, R., Strimas-Mackey, M., Morrell, N., Edwards, B. P. M., Arcese, P., Bennett, J. R., & Possingham, H. P. (2025). Systematic conservation prioritization with the prioritizr R package. Conservation Biology, 39(1), e14376. https://doi.org/10.1111/cobi.14376

Harlio, A., Kuussaari, M., Heikkinen, R. K., & Arponen, A. (2019). Incorporating landscape heterogeneity into multi-objective spatial planning improves biodiversity conservation of semi-natural grasslands. Journal for Nature Conservation, 49, 37-44. https://doi.org/10.1016/j.jnc.2019.01.003

Hermoso, V., Bota, G., Brotons, L., & Morán-Ordóñez, A. (2023). Addressing the challenge of photovoltaic growth: Integrating multiple objectives towards sustainable green energy development. Land Use Policy, 128, 106592. https://doi.org/10.1016/j.landusepol.2023.106592

Hildemann, M., Pebesma, E., & Verstegen, J. A. (2023). Multi-objective Allocation Optimization of Soil Conservation Measures Under Data Uncertainty. Environmental Management, 72(5), 959-977. https://doi.org/10.1007/s00267-023-01837-6

Holl, K. D., & Aide, T. M. (2011). When and where to actively restore ecosystems? *Forest Ecology and Management*, 261(10), 1558–1563. https://doi.org/10.1016/j.foreco.2010.07.004

Iglesias, M. C., Hermoso, V., Campos, J. C., Carvalho-Santos, C., Fernandes, P. M., Freitas, T. R., Honrado, J. P., Santos, J. A., Sil, Â., Regos, A., & Azevedo, J. C. (2022). Climate- and fire-smart landscape scenarios call for redesigning protection regimes to achieve multiple management goals. Journal of Environmental Management, 322, 116045. https://doi.org/10.1016/j.jenvman.2022.116045

IPBES (Intergovernmental Science-Policy Platform on Biodiversity and Ecosystem Services). (2018) The IPBES assessment report on land degradation and restoration. Intergovernmental Science-Policy Platform on Biodiversity and Ecosystem Services, Bonn, Germany

IPBES (Intergovernmental Science-Policy Platform on Biodiversity and Ecosystem Services). (2019). *Summary for policymakers of the global assessment report on biodiversity and ecosystem services of the Intergovernmental Science-Policy Platform on Biodiversity and Ecosystem Services* (S. Díaz, J. Settele, E. S. Brondizio, H. T. Ngo, M. Guèze, J. Agard, ... & C. N. Zayas, Eds.). IPBES secretariat. https://doi.org/10.5281/zenodo.3553579

IPCC (2022) Climate change 2022: impacts, adaptation, and vulnerability. Contribution of Working Group II to the Sixth Assessment Report of the Intergovernmental Panel on Climate Change. Cambridge University Press, Cambridge, UK and New York, NY, USA

IUCN (International Union for Conservation of Nature) (2022) Decade on Ecosystem Restoration 2021–2030: Policy Brief. Retrieved from https://www.decadeonrestoration.org/

Jung, M., Arnell, A., De Lamo, X., García-Rangel, S., Lewis, M., Mark, J., Merow, C., Miles, L., Ondo, I., Pironon, S., Ravilious, C., Rivers, M., Schepaschenko, D., Tallowin, O., Van Soesbergen, A., Govaerts, R., Boyle, B. L., Enquist, B. J., Feng, X., … Visconti, P. (2021). Areas of global importance for conserving terrestrial biodiversity, carbon and water. Nature Ecology & Evolution, 5(11), 1499-1509. https://doi.org/10.1038/s41559-021-01528-7

Justeau-Allaire, D., Hanson, J. O., Lannuzel, G., Vismara, P., Lorca, X., & Birnbaum, P. (2023). restoptr: an R package for ecological restoration planning. Restoration Ecology, 31(5), e13910.

Kramer, D. B., Zhang, T., Cheruvelil, K. S., Ligmann-Zielinska, A., & Soranno, P. A. (2013). A Multi-objective, Return on Investment Analysis for Freshwater Conservation Planning. Ecosystems, 16(5), 823-837. https://doi.org/10.1007/s10021-013-9654-3

Kukkala, A. S., & Moilanen, A. (2013). Core concepts of spatial prioritisation in systematic conservation planning. Biological Reviews, 88(2), 443-464. https://doi.org/10.1111/brv.12008

Lara A, Little C, Urrutia R, McPhee J, Álvarez-Garretón C, Oyarzún C, Soto D, Donoso P, Nahuelhual L, Pino M, Arismendi I (2009) Assessment of ecosystem services as an opportunity for the conservation and management of native forests in Chile. *Forest Ecology and Management* 258:415–424

Lemos, C. M. G., Beyer, H. L., Runting, R. K., Andrade, P. R., & Aguiar, A. P. D. (2023). Multicriteria optimization to develop cost-effective pes-schemes to restore multiple environmental benefits in the Brazilian Atlantic Forest. Ecosystem Services, 60, 101515. https://doi.org/10.1016/j.ecoser.2023.101515

Little C, Cuevas JG, Lara A, Pino M, Schoenholtz S (2015) Buffer effects of streamside native forests on water provision in watersheds dominated by exotic forest plantations. *Ecohydrology* 8:1205–1217

López-Cubillos, S., Runting, R. K., Suárez-Castro, A. F., Williams, B. A., Armenteras, D., Manuel Ochoa-Quintero, J., & McDonald-Madden, E. (2022). Spatial prioritization to achieve the triple bottom line in Payment for ecosystem services design. Ecosystem Services, 55, 101424. https://doi.org/10.1016/j.ecoser.2022.101424

Luebert F, Pliscoff P (2017) Sinópsis bioclimática y vegetacional de Chile. Editorial Universitaria, Santiago, Chile

Margules CR, Pressey RL (2000) Systematic conservation planning. *Nature* 405(6783):243–247

Margules, C. R., & Sarkar, S. (2007). Systematic conservation planning. Cambridge University Press.

Martin, A. E., Neave, E., Kirby, P., Drever, C. R., & Johnson, C. A. (2022). Multi-objective optimization can balance trade-offs among boreal caribou, biodiversity, and climate change objectives when conservation hotspots do not overlap. Scientific Reports, 12(1), 11895. https://doi.org/10.1038/s41598-022-15274-8

Mazziotta, A., Podkopaev, D., Triviño, M., Miettinen, K., Pohjanmies, T., & Mönkkönen, M. (2017). Quantifying and resolving conservation conflicts in forest landscapes via multiobjective optimization. Silva Fennica, 51(1). https://doi.org/10.14214/sf.1778

McIntosh, E. J., Pressey, R. L., Lloyd, S., Smith, R. J., & Grenyer, R. (2017). The Impact of Systematic Conservation Planning. Annual Review of Environment and Resources, 42(1), 677-697. https://doi.org/10.1146/annurev-environ-102016-060902

MEA (Millennium Ecosystem Assessment) (2005) Ecosystems and human well-being: synthesis. Island Press, Washington D.C.

Menz MH, Dixon KW, Hobbs RJ (2013) Hurdles and opportunities for landscape-scale restoration. *Science* 339(6119):526–529

Ministry of Environment Chile (2023) Plan Nacional de Restauración de Paisajes 2020–2030. Ministerio del Medio Ambiente de Chile, Santiago, Chile. Retrieved from https://mma.gob.cl

Miranda A, Altamirano A, Cayuela L, Pincheira F, Lara A (2015) Different times, same story: native forest loss and landscape homogenization in three physiographical regions of central Chile. *Applied Geography* 60:20–28

Moilanen, A., Lehtinen, P., Kohonen, I., Jalkanen, J., Virtanen, E. A., & Kujala, H. (2022). Novel methods for spatial prioritization with applications in conservation, land use planning and ecological impact avoidance. Methods in Ecology and Evolution, 13(5), 1062-1072. https://doi.org/10.1111/2041-210X.13819

Morales-Barbero, J., & Ferrer-Castán, D. (2019). Using a goal programming approach to design and evaluate protected areas for the conservation of multiple dimensions of biodiversity. Journal for Nature Conservation, 49, 54-62. https://doi.org/10.1016/j.jnc.2019.01.007

Moreno-Faguett, M., Salgado-Rojas, J., Castillo-Mandujano, J., Larraín-Barrios, B., Martínez-Harms, M. J., Hermoso, V., & Álvarez-Miranda, E. (2026). Data and Code for "Exact ε-Constraint Optimization for Spatial Planning: Balancing Species Risk Distribution in Ecological Restoration" (v1.0.0) [Data set]. Zenodo. https://doi.org/10.5281/zenodo.20412422

Myers N, Mittermeier RA, Mittermeier CG, da Fonseca GA, Kent J (2000) Biodiversity hotspots for conservation priorities. *Nature* 403(6772):853–858

Neubert, S., McGowan, J., Metcalfe, K., Hanson, J. O., Buenafe, K. C. V., Dabalà, A., Dunn, D. C., Everett, J. D., Possingham, H. P., Stelzenmüller, V., Estep, A., Ervin, J., & Richardson, A. J. (2025). Multiple-use spatial planning for sustainable development and conservation. Trends in Ecology & Evolution, S0169534725002538. https://doi.org/10.1016/j.tree.2025.09.007

NYDF (New York Declaration on Forests) (2024) Forest Declaration Platform. Retrieved from https://forestdeclaration.org

Orrego G, Espíndola L, Pogorelow B, Leal J, Morales C, Saa R (2023) Informe País: Estado del Medio Ambiente en Chile 2022. Resumen para tomadores de decisiones. Ministerio del Medio Ambiente, Santiago, Chile

Orsi F, Geneletti D, Newton AC (2011) Towards a common set of criteria and indicators to identify forest restoration priorities: An expert panel-based approach. Ecological Indicators 2:337-347

Orsi, F., & Geneletti, D. (2010). Identifying priority areas for Forest Landscape Restoration in Chiapas (Mexico): An operational approach combining ecological and socioeconomic criteria. Landscape and Urban Planning, 94, 20–30. doi:10.1016/j.landurbplan.2009.07.014

Palomo, I., Dujardin, Y., Midler, E., Robin, M., Sanz, M. J., & Pascual, U. (2019). Modeling trade-offs across carbon sequestration, biodiversity conservation, and equity in the distribution of global REDD+ funds. Proceedings of the National Academy of Sciences, 116(45), 22645-22650. https://doi.org/10.1073/pnas.1908683116

Pliscoff P, Fuentes-Castillo T (2011) Representativeness of terrestrial ecosystems in Chile's protected area system. *Environmental Conservation* 38(3):303–311

Pliscoff P, Luebert F, Hilger HH, Guisan A (2014) Effects of alternative sets of climatic predictors on species distribution models and associated estimates of extinction risk: a test with plants in an arid environment. *Ecological Modelling* 288:166–177

Pliscoff, P., Zambrana-Torrelio, C., Zambrano, S., Ferrer-Paris, J. R., Rodríguez-Clark, K., Rodríguez, J. P., Keith, D., Simonetti, J., Luebert, F., & Asmüssen, M. (2025). IUCN terrestrial ecosystem risk assessment for Chile. Conservation Letters. *In review*.

Pressey, R.L., Humphries, C.J., Margules, C.R., Vane-Wright, R.I. & Williams, P.H. 1993. Beyond opportunism: Key principles for systematic reserve selection. Trends in Ecology & Evolution 8: 124-128.

Pressey, R. L., Johnson, I. R., & Wilson, P. D. (1994). Shades of irreplaceability: towards a measure of the contribution of sites to a reservation goal. *Biodiversity & Conservation*, 3(3), 242–262.

Sala, E., Mayorga, J., Bradley, D., Cabral, R. B., Atwood, T. B., Auber, A., Cheung, W., Costello, C., Ferretti, F., Friedlander, A. M., Gaines, S. D., Garilao, C., Goodell, W., Halpern, B. S., Hinson, A., Kaschner, K., Kesner-Reyes, K., Leprieur, F., McGowan, J., … Lubchenco, J. (2021). Protecting the global ocean for biodiversity, food and climate. Nature, 592(7854), 397-402. https://doi.org/10.1038/s41586-021-03371-z

Sangüesa C, Pizarro R, Ingram B, Balocchi F, García-Chevesich P, Pino J, Ibáñez A, Vallejos C, Mendoza R, Bernal A, Valdés-Pineda R, Pérez F (2023) Streamflow trends in central Chile. *Hydrology* 10(7):144

Santoro M, Cartus O (2024) ESA Biomass Climate Change Initiative (Biomass_cci): global datasets of forest above-ground biomass for the years 2010, 2015, 2016, 2017, 2018, 2019, 2020, and 2021, v5. NERC EDS Centre for Environmental Data Analysis

Scherson, R.A., Albornoz, A.A., Moreira-Munoz, A.S. & Urbina-Casanova, R. 2014. Endemicity and evolutionary value: a study of Chilean endemic vascular plant genera. Ecol Evol 4: 806-816. https://doi.org/10.1002/ece3.960

Scherson, R.A., Thornhill, A.H., Urbina-Casanova, R., Freyman, W.A., Pliscoff, P.A. & Mishler, B.D. 2017. Spatial phylogenetics of the vascular flora of Chile. Molecular Phylogenetics and Evolution 112: 88-95. https://doi.org/10.1016/j.ympev.2017.04.021

Schlottfeldt, S., Walter, M. E. M. T., L.F. Carvalho, A. C. P., Soares, T. N., Telles, M. P. C., Loyola, R. D., & Diniz-Filho, J. A. F. (2015). Multi-objective optimization in systematic conservation planning and the representation of genetic variability among populations. Genetics and Molecular Research, 14(2), 6744-6761. https://doi.org/10.4238/2015.June.18.18

Schüler, J., & Bustamante, M. M. C. (2022). Spatial planning for restoration in Cerrado: Balancing the trade-offs between conservation and agriculture. Journal of Applied Ecology, 59(10), 2616-2626. https://doi.org/10.1111/1365-2664.14262

Schulz JJ, Cayuela L, Echeverría C, Salas J, Rey-Benayas JM (2010) Monitoring land cover change of the dryland forest landscape of central Chile (1975–2008). *Applied Geography* 30(3):436–447

Schuster, R., Buxton, R., Hanson, J. O., Binley, A. D., Pittman, J., Tulloch, V., La Sorte, F. A., Roehrdanz, P. R., Verburg, P. H., Rodewald, A. D., Wilson, S., Possingham, H. P., & Bennett, J. R. (2023). Protected area planning to conserve biodiversity in an uncertain future. Conservation Biology, 37(3), e14048. https://doi.org/10.1111/cobi.14048

Schuster, R., Hanson, J. O., Strimas-Mackey, M., & Bennett, J. R. (2020). Exact integer linear programming solvers outperform simulated annealing for solving conservation planning problems. PeerJ, 8, e9258. https://doi.org/10.7717/peerj.9258

Sewall, B. J., Freestone, A. L., Moutui, M. F. E., Toilibou, N., Saïd, I., Toumani, S. M., Attoumane, D., & Iboura, C. M. (2011). Reorienting Systematic Conservation Assessment for Effective Conservation Planning: Assessment and Conservation Planning. Conservation Biology, 25(4), 688-696. https://doi.org/10.1111/j.1523-1739.2011.01697.x

Sirko, W., Kashubin, S., Ritter, M., Annkah, A., Bouchareb, Y. S. E., Dauphin, Y., Keysers, D., Neumann, M., Cisse, M., & Quinn, J. (2021). Continental-scale building detection from high resolution satellite imagery. arXiv. https://arxiv.org/abs/2107.12283

Smith-Ramirez C, Castillo-Mandujano J. Becerra P, Sandoval N, Allende R, Fuentes R, Acuña MA (2022) Combining remote sensing and field data to assess recovery of the Chilean Mediterranean vegetation after fire: Effect of time elapsed and burn severity. Forest Ecology and Management 503:119800

Srivathsa, A., Vasudev, D., Nair, T., Chakrabarti, S., Chanchani, P., DeFries, R., Deomurari, A., Dutta, S., Ghose, D., Goswami, V. R., Nayak, R., Neelakantan, A., Thatte, P., Vaidyanathan, S., Verma, M., Krishnaswamy, J., Sankaran, M., & Ramakrishnan, U. (2023). Prioritizing India's landscapes for biodiversity, ecosystem services and human well-being. Nature Sustainability, 6(5), 568-577. https://doi.org/10.1038/s41893-023-01063-2

Strassburg, B. B. N., Beyer, H. L., Crouzeilles, R., Iribarrem, A., Barros, F., De Siqueira, M. F., Sánchez-Tapia, A., Balmford, A., Sansevero, J. B. B., Brancalion, P. H. S., Broadbent, E. N., Chazdon, R. L., Filho, A. O., Gardner, T. A., Gordon, A., Latawiec, A., Loyola, R., Metzger, J. P., Mills, M., … Uriarte, M. (2018). Strategic approaches to restoring ecosystems can triple conservation gains and halve costs. Nature Ecology & Evolution, 3(1), 62-70. https://doi.org/10.1038/s41559-018-0743-8

Strassburg, B. B. N., Iribarrem, A., Beyer, H. L., Cordeiro, C. L., Crouzeilles, R., Jakovac, C. C., Braga Junqueira, A., Lacerda, E., Latawiec, A. E., Balmford, A., Brooks, T. M., Butchart, S. H. M., Chazdon, R. L., Erb, K.-H., Brancalion, P., Buchanan, G., Cooper, D., Díaz, S., Donald, P. F., … Visconti, P. (2020). Global priority areas for ecosystem restoration. Nature, 586(7831), 724-729. https://doi.org/10.1038/s41586-020-2784-9

Strauch, M., Cord, A. F., Pätzold, C., Lautenbach, S., Kaim, A., Schweitzer, C., Seppelt, R., & Volk, M. (2019). Constraints in multi-objective optimization of land use allocation – Repair or penalize? Environmental Modelling & Software, 118, 241-251. https://doi.org/10.1016/j.envsoft.2019.05.003

Tessler N, Wittenberg L, Greenbaum N (2016) Vegetation cover and species richness after recurrent forest fires in the Eastern Mediterranean ecosystem of Mount Carmel, Israel. *Science of The Total Environment* 572:1395–1402

Thomas C, Cameron A, Green RE, Bakkenes M, Beaumont LJ, Collingham YC, Erasmus BF, Ferreira de Siqueira M, Grainger A, Hannah L, Hughes L, Huntley B, van Jaarsveld AS, Midgley GF, Miles L, Ortega-Huerta MA, Peterson AT, Phillips OL, Williams SE (2004) Extinction risk from climate change. *Nature* 427:145–150

Thuiller, W., Lafourcade, B., Engler, R., & Araújo, M. B. (2009). BIOMOD–a platform for ensemble forecasting of species distributions. Ecography, 32(3), 369-373.

Thuiller, W., Georges, D., Engler, R., Breiner, F., Georges, M. D., & Thuiller, C. W. (2016). Package 'biomod2'. Species distribution modeling within an ensemble forecasting framework, 10(1600), 0587.

Úmeda X, Sarricolea P (2016) Wildfires in Chile: a review. *Global and Planetary Change* 146:152–162

UNFCCC (United Nations Framework Convention on Climate Change) (2018) Chile's Third Biennial Update Report. Ministry of Environment, Santiago, Chile

United Nations (2024) UN Decade on Ecosystem Restoration 2021–2030. Retrieved from https://www.decadeonrestoration.org

Vargas-Ríos OR, Vargas-Villegas RF, Bonilla-Moheno M (2014) Las especies invasoras: un reto para la restauración ecológica. *Revista de Ciencias Ambientales* 39(1):23–34

Vilà, M., Espinar, J. L., Hejda, M., Hulme, P. E., Jarošík, V., Maron, J. L., Pergl, J., Schaffner, U., & Pyšek, P. (2011). Ecological impacts of invasive alien plants: A meta-analysis of their effects on species, communities and ecosystems. Ecology Letters, 14(7), 702–708. https://doi.org/10.1111/j.1461-0248.2011.01628.x

Watts, M. E., Ball, I. R., Stewart, R. S., Klein, C. J., Wilson, K., Steinback, C., Lourival, R., Kircher, L., & Possingham, H. P. (2009). Marxan with Zones: Software for optimal conservation based land- and sea-use zoning. Environmental Modelling & Software, 24(12), 1513-1521. https://doi.org/10.1016/j.envsoft.2009.06.005

Wiersma, Y. F., & Sleep, D. J. H. (2016). A review of applications of the six-step method of systematic conservation planning. The Forestry Chronicle, 92(03), 322-335. https://doi.org/10.5558/tfc2016-059

Williams, B. A., Archibald, C. L., Brazill-Boast, J., Drielsma, M. J., Thapa, R., Love, J., Cho, F. H. T., Lunney, D., Fitzsimons, J. A., Iftekhar, M. S., Villarreal-Rosas, J., Bekessy, S., Hetherington, S. B., McAlpine, C. A., Beaumont, L. J., Thonell, J., & Rhodes, J. R. (2024). Optimal investments in private land conservation depend more on landholder preferences than climate change. Environmental Research Letters, 19(12), 124047. https://doi.org/10.1088/1748-9326/ad8d6b

Williams, B. A., Grantham, H. S., Watson, J. E. M., Alvarez, S. J., Simmonds, J. S., Rogéliz, C. A., Da Silva, M., Forero-Medina, G., Etter, A., Nogales, J., Walschburger, T., Hyman, G., & Beyer, H. L. (2020). Minimising the loss of biodiversity and ecosystem services in an intact landscape under risk of rapid agricultural development. Environmental Research Letters, 15(1), 014001. https://doi.org/10.1088/1748-9326/ab5ff7

Williams, B. A., López-Cubillos, S., Ochoa-Quintero, J. M., Crouzeilles, R., Villa-Piñeros, M., Isaacs Cubides, P. J., Schmoeller, M., Marin, W., Tedesco, A., Bastos, D., Suárez-Castro, A. F., Romero Jiménez, L. H., Broadbent, E. N., Almeyda Zambrano, A. M., Vincent, J. R., Yi, Y., Chazdon, R. L., Watson, J. E. M., Urbano, E. A. N., … Beyer, H. L. (2024). Bringing the forest back: Restoration priorities in Colombia. Diversity and Distributions, 30(4), e13821. https://doi.org/10.1111/ddi.13821

Williams, P. J., & Kendall, W. L. (2017). A guide to multi-objective optimization for ecological problems with an application to cackling goose management. Ecological Modelling, 343, 54-67. https://doi.org/10.1016/j.ecolmodel.2016.10.010

Zamorano-Elgueta, C., Orsi, F., Geneletti, D., Cayuela, L., Hamer, R., Lara, A., & Benayas, J. M. R. (2025). Integrating Ecological Suitability and Socioeconomic Feasibility at Landscape Scale to Restore Biodiversity and Ecosystem Services in Southern Chile. Environmental Management, 75(3), 588-605. https://doi.org/10.1007/s00267-024-02103-z

# Navigating Spatial Trade-offs in Restoration Planning: A Multi-Objective Optimization Framework Integrating Ecological Feasibility

# Supplementary Material

## Summary

**Appendix A** presents the mathematical formulation of the multi-objective optimization framework, including the mixed-integer linear programming structure and the piecewise-linear approximation of the species–area relationship used to model extinction risk reduction.

**Appendix B** describes the computational implementation of the optimization models, including solver settings, model size, presolve behavior, runtime performance, and numerical stability considerations.

**Appendix C** provides supplementary results and spatial diagnostics, including latitudinal statistics, objective-level performance matrices, and national-scale summaries of selection frequency and functional roles of planning units.

# Appendix A. Mathematical formulation of the multi-objective optimization framework

## A.1 Notation, sets, indices, decision variables, and parameters

This appendix provides the complete mathematical formulation of the optimization framework introduced in **Section 2** of the Methods. The notation below consolidates all sets, indices, decision variables, and parameters used throughout both Step 1 (single-objective optimization; **Section 2.4**) and Step 2 (multi-objective goal programming; **Section 2.5**).

**Sets and indices**

Let:

- $\mathcal{I}$ denote the set of units, indexed by $i$.
- $\mathcal{I}^{\text{unsuit}} \subseteq \mathcal{I}$ denote the set of units excluded (locked-out) by the land-suitability mask, i.e., units that are not eligible for restoration.
- $\mathcal{S}$ denote the set of species, indexed by $s$.
- $\mathcal{J}$ denote the set of optimization criteria, indexed by $j$, considered in the goal programming formulation.
- $\mathcal{K}$ denote the set of breakpoints, indexed by $k$, used in the piecewise-linear (PWL) approximation of the species–area relationship (SAR) term.

**Decision variables**

For each $i \in \mathcal{I}$, define the binary decision variable

$$x_i = \begin{cases} 1, & if\ unit\ i\ is\ selected\ for\ restoration \\ 0, & otherwise \end{cases} \quad \text{(A.1)}$$

Collectively, $\mathbf{x} = (x_i)_{i \in \mathcal{I}} \in \{0,1\}^{|\mathcal{I}|}$ defines a restoration plan.

For the extinction risk formulation, and for each species $s \in \mathcal{S}$, define:

- $q_s$: projected species–area ratio under restoration plan **x**.
- $\psi_s$: auxiliary continuous variable representing the piecewise-linear approximation of $q_s^{\alpha}$.
- $e_s$: projected extinction risk under restoration plan **x**.

For the goal programming model, and for each criterion $j \in \mathcal{J}$, define:

- $\delta_j^-$: underachievement (negative deviation) from target $G_j$.
- $\delta_j^+$: overachievement (positive deviation) from target $G_j$.

**Parameters**

For each unit $i \in \mathcal{I}$ and species $s \in \mathcal{S}$, let:

- $a_i$ be the area of planning unit $i$.

- $a_{is}$ be the contribution of unit $i$ to species $s$, measured as the area of overlap between unit $i$ and the habitat of species $s$.
- $c_i$ be the carbon storage value associated with unit $i$.
- $w_i$ be the water provision value associated with unit $i$.
- $f_i$ be the restoration feasibility value associated with unit $i$.

For each species $s \in \mathcal{S}$, let:

- $a_s^0$ be the current area of species $s$.
- $A_s^0$ be the reference (e.g., pre-settlement) habitat area of species $s$.
- $e_s^0$ be the baseline extinction risk of species $s$, computed consistently with the SAR formulation based on current habitat conditions.
- $q_s^{\max}$ be an upper bound on $q_s$, defined as

$$q_s^{\max} = \frac{a_s^0 + \sum_{i \in \mathcal{J} \setminus \mathcal{J}^{\text{unsuit}}} a_{is}}{A_s^0}$$

  i.e., the species–area ratio obtained if all eligible restoration units are selected.

- $\alpha$ be the species–area relationship exponent.

At the landscape level, let:

- $A$ be the total area of the study region.
- $t_A$ be the restoration area budget expressed as a fraction of total area.

For the PWL approximation, and for each breakpoint $b \in \mathcal{B}$, let:

- $\xi_k$ denote the abscissa (breakpoint location) of breakpoint $k$.
- $\eta_k$ denote the corresponding ordinate value, with $\eta_k = \min\{\xi_k^{\alpha}, 1\}$

For each criterion $j \in \mathcal{J}$, let:

- $G_j$ be the target value associated with criterion $j$, defined as the optimal value of the corresponding single-objective problem.
- $\omega_j$ be the weight assigned to criterion $j$.

## A.2. Common feasible region

All optimization problems are defined over the same feasible set $\Phi \subseteq \{0,1\}^{|\mathcal{J}|}$, determined by the restoration budget and land suitability constraints described in **Section 2.3** of the Methods. Specifically,

$$\Phi = \left\{ \mathbf{x} \in \{0,1\}^{|\mathcal{I}|} : \sum_{i \in \mathcal{I}} a_i x_i \leq t_A A \, , x_i = 0 \; \forall i \in \mathcal{I}^{\text{unsuit}} \right\} \tag{A.2}$$

Equivalently, the common constraints can be written explicitly as

$$\sum_{i \in I} a_i x_i \leq t_A A \tag{A.3}$$

$$x_i = 0, \qquad \forall i \in \mathcal{I}^{\text{unsuit}} \tag{A.4}$$

$$x_i \in \{0,1\}, \qquad \forall i \in \mathcal{I} \tag{A.5}$$

Constraint (A.3) is the restoration budget constraint (Eq. (1) in the Methods), and constraint (A.4) is the land suitability constraint (Eq. (2) in the Methods). Constraint (A.5) enforces the binary nature of the decision variables. All single-objective and multi-objective formulations share this feasible region; therefore, differences among solutions arise from the optimized criterion or set of criteria, rather than from changes in feasibility conditions.

### A.3. Projected species–area ratio and extinction risk

The biodiversity criterion is based on the reduction in species extinction risk induced by restoration. For each species $s \in \mathcal{S}$, the increase in habitat induced by a restoration plan $\mathbf{x}$ is

$$a_s(\mathbf{x}) = \sum_{i \in \mathcal{I}} a_{is} x_i \tag{A.6}$$

Hence, the projected species–area ratio is

$$q_s(\mathbf{x}) = \frac{a_s^0 + a_s(\mathbf{x})}{A_s^0} = \frac{a_s^0 + \sum_{i \in \mathcal{I}} a_{is} x_i}{A_s^0}, \qquad \forall s \in \mathcal{S} \tag{A.7}$$

This provides an explicit linear expression of $q_s(\mathbf{x})$ in terms of the decision variables. For simplicity, we write $q_s \equiv q_s(\mathbf{x})$ whenever no ambiguity arises.

Under the SAR formulation, projected extinction risk is

$$e_s(\mathbf{x}) = 1 - \min\{q_s^{\alpha}, 1\}, \qquad \forall s \in \mathcal{S} \tag{A.8}$$

This formulation ensures that extinction risk is bounded in $[0,1]$. Because $q_s$ may exceed 1 when restored habitat plus current habitat exceeds the reference area $A_s^0$, the SAR term is capped at 1 to maintain ecological consistency.

### A.4. PWL approximation of the SAR term

To preserve linearity of the optimization problem, the nonlinear function $q_s^{\alpha}$ is approximated using a piecewise-linear representation over a finite set of breakpoints $\mathcal{K}$ spanning the relevant domain of $q_s$, as described in **Section 2.4.1** of the Methods.

The breakpoint abscissae $\xi_k, k \in \mathcal{K}$, are constructed over the interval $[0,1]$ as

$$\xi_k = \left(\frac{k-1}{|\mathcal{K}|-1}\right)^{1/\alpha}, \qquad k = 1, \dots, |\mathcal{K}| \tag{A.9}$$

with corresponding ordinate values

$$\eta_k = \min\{\xi_k^{\alpha}, 1\}, \qquad k = 1, \dots, |\mathcal{K}| \tag{A.10}$$

This construction allocates breakpoints according to the curvature of the SAR function. In the reported experiments, the chosen approximation tolerance $\tau = 0.05$ (5%) yields $|\mathcal{K}| = 28$ breakpoints (27 segments). For all breakpoints with $\xi_k \geq 1, \eta_k = 1$, thus producing a flat segment consistent with the capped SAR function.

If $\max_{s\in\mathcal{S}} q_s^{\max} > 1$, an additional breakpoint is appended at $q = \max_{s\in\mathcal{S}} q_s^{\max}$, and the PWL representation remains capped at 1 to preserve consistency with the bounded definition of extinction risk.

For each species $s \in \mathcal{S}$, the variable $q_s$ is bounded within the domain of the PWL representation, i.e., $0 \leq q_s \leq q_s^{\max}$.

The pair $(q_s, \psi_s)$ is then constrained to lie on the piecewise-linear approximation of the function $q \to \min(q^{\alpha}, 1)$. Accordingly, $\psi_s$ represents the PWL approximation of $\min(q_s^{\alpha}, 1)$, i.e.,

$$\psi_s = \mathrm{PWL}(q_s), \qquad \forall s \in \mathcal{S} \tag{A.11}$$

where PWL(·) denotes the piecewise-linear approximation of $f(q) = \min\{q^{\alpha}, 1\}$. This representation is implemented in practice using solver-specific general constraints (e.g., Gurobi's `addGenConstrPWL()`).

Finally, the projected extinction risk is computed as

$$e_s(\mathbf{x}) = 1 - \psi_s, \qquad \forall s \in \mathcal{S} \tag{A.12}$$

This linearization introduces one continuous variable $q_s$ and one auxiliary continuous variable $\psi_s$ per species, as well as one PWL general constraint per species (see Table B1).

## A.5. Single-objective formulations (Step 1)

As described in **Section 2.4** of the Methods, Step 1 consists of optimizing each criterion independently over the common feasible set Φ. The resulting optimal values define the ideal point used subsequently in the goal programming model.

**Extinction risk reduction**

Using the biodiversity representation in (A.7) and (A.11)–(A.12), the extinction risk reduction problem can be written as

$$\mathbf{z}_E^* = \max \sum_{s\in\mathcal{S}} (e_s^0 - e_s) \tag{A.13}$$

subject to

$$q_s = \frac{a_s^0 + \sum_{i \in \mathcal{J}} a_{is} x_i}{A_s^0}, \qquad \forall s \in \mathcal{S} \tag{A.14}$$

$$\psi_s = \mathrm{PWL}(q_s), \qquad \forall s \in \mathcal{S} \tag{A.15}$$

$$e_s = 1 - \psi_s, \qquad \forall s \in \mathcal{S} \tag{A.16}$$

and constraints (A.3)–(A.5). This formulation corresponds to Eq. (3) in the Methods, expressed here using a PWL approximation within a MILP framework.

**Carbon storage**

The carbon storage problem is

$$\mathbf{z}_c^* = \max \sum_{i \in \mathcal{J}} c_i x_i \tag{A.17}$$

subject to constraints (A.3)–(A.5). This formulation corresponds to Eq. (4) in the Methods.

**Water provision**

The water provision problem is

$$\mathbf{z}_w^* = \max \sum_{i \in \mathcal{J}} w_i x_i \tag{A.18}$$

subject to constraints (A.3)–(A.5). This formulation corresponds to Eq. (5) in the Methods.

**Restoration feasibility**

The restoration feasibility problem is

$$\mathbf{z}_f^* = \max \sum_{i \in \mathcal{J}} f_i x_i \tag{A.19}$$

subject to constraints (A.3)–(A.5). This formulation corresponds to Eq. (6) in the Methods.

## A.6. Multi-objective formulation (Step 2)

Step 2 seeks a compromise solution that minimizes normalized deviations from the single-objective optima obtained in Step 1. For each $j \in \mathcal{J}$, the target value is defined as

$$G_j = \mathbf{z}_j^*, \qquad \forall j \in \mathcal{J} \tag{A.20}$$

where $\mathbf{z}_j^*$ is the optimal value of the corresponding single-objective problem.

Consistent with **Section 2.5** of the Methods, the achievement levels for each criterion $j$ are

$$b_E(\mathbf{x}) = \sum_{s \in \mathcal{S}} (e_s^0 - e_s) \tag{A.21}$$

$$b_c(\mathbf{x}) = \sum_{i \in \mathcal{J}} c_i x_i \tag{A.22}$$

$$b_w(\mathbf{x}) = \sum_{i \in \mathcal{I}} w_i x_i \tag{A.23}$$

$$b_f(\mathbf{x}) = \sum_{i \in \mathcal{I}} f_i x_i \tag{A.24}$$

Deviations from these targets are represented by the standard goal constraint (Eq. (7) in the Methods)

$$b_j(\mathbf{x}) - \delta_j^+ + \delta_j^- = G_j, \qquad \forall j \in \mathcal{J} \tag{A.25}$$

**General GP model**

The general weighted normalized goal programming model is then

$$\mathbf{g}^* = \min \sum_{j \in \mathcal{J}} \omega_j \left( \frac{\delta_j^+ + \delta_j^-}{G_j} \right) \tag{A.26}$$

subject to

$$\sum_{s \in \mathcal{S}} (e_s^0 - e_s) - \delta_E^+ + \delta_E^- = G_E \tag{A.27}$$

$$\sum_{i \in \mathcal{I}} c_i x_i - \delta_c^+ + \delta_c^- = G_c \tag{A.28}$$

$$\sum_{i \in \mathcal{I}} w_i x_i \ - \delta_w^+ + \delta_w^- = G_w \tag{A.29}$$

$$\delta_j^+, \delta_j^- \geq 0, \qquad \forall j \in \mathcal{J} \tag{A.30}$$

and, when $f \in \mathcal{J}$

$$\sum_{i \in \mathcal{I}} f_i x_i - \delta_f^+ + \delta_f^- = G_f \tag{A.31}$$

together with constraints (A.3)–(A.5) and the biodiversity PWL constraints (A.14)–(A.16).

**Simplified GP model**

Because each target $G_j = \mathbf{z}_j^*$ is the maximum achievable value of criterion $j$ over the feasible set $\Phi$, no feasible solution can exceed its corresponding target. Hence,

$$b_j(\mathbf{x}) \leq G_j, \qquad \forall j \in \mathcal{J}, \ \ \forall \mathbf{x} \in \Phi \tag{A.32}$$

which implies that $\delta_j^+ = 0$ at optimality (assuming $G_j > 0$ for all $j \in \mathcal{J}$). Under this property, the formulation simplifies to (Eq. (8) in the Methods)

$$\mathbf{g}^* = \min \sum_{j \in \mathcal{J}} \frac{\delta_j^-}{G_j} \tag{A.33}$$

subject to constraints (A.3)–(A.5), (A.27)–(A.31), and the PWL biodiversity constraints (A.14)–(A.16).

In the reported experiments, all weights were set to unity, $\omega_j = 1$ for all $j \in \mathcal{J}$, yielding the neutral baseline formulation described in **Section 2.5** of the Methods. Under this specification, the model minimizes the normalized L1-distance to the ideal point.

**Feasibility-excluded and feasibility-included scenarios**

The two multi-objective scenarios considered in **Section 2.6** are obtained by changing only the index set $\mathcal{J}$:

- **Feasibility-excluded formulation:**

$$\mathcal{J}^{\mathrm{F-ex}} = \{E, c, w\} \tag{A.34}$$

- **Feasibility-included formulation:**

$$\mathcal{J}^{\mathrm{F-in}} = \{E, c, w, f\} \tag{A.35}$$

Both scenarios share the same feasible region and differ only in whether restoration feasibility is included as an explicit optimization criterion.

## Appendix B. Computational implementation and performance

**Solver settings.** All MILP formulations were implemented in a unified pipeline and solved using Gurobi Optimizer v11.0.2 (win64) on Windows 10. Experiments were executed on an 11th Gen Intel(R) Core(TM) i7-1165G7 @ 2.80 GHz CPU (4 physical cores, 8 logical processors), using up to 8 threads. For numerical stability, we set NumericFocus = 3 and ScaleFlag = 2. A relative optimality tolerance of MIPGap = 0.01 (1%) was enforced for all models; in practice, all runs terminated with substantially tighter gaps (≤0.001%, as reported in the solver logs). All remaining solver parameters were left at their default values.

**Decision space and eligibility masking.** The national planning grid contains 812,910 1 $km^2$ planning units. After applying the land suitability constraint (**Section 2.3**), 632,612 $km^2$ remained suitable for restoration. To preserve a consistent national planning grid across all formulations, all units were included in the index set, while unsuitable units were excluded by fixing their binary decision variables to zero ($x_i = 0$), thereby restricting the feasible set to eligible units, as enforced by Eq. (2) in the Methods and constraint (A.4) in Appendix A.

**Model size and computational implications.** Across runs, full models contained 180,300–180,767 constraints and 812,910–813,381 variables, with ~1.42–14.64 million nonzero coefficients, depending on the objective set. The three linear single-objective formulations (carbon storage, water provision, and restoration feasibility; Eqs. (4)–(6)) yielded purely binary models with 812,910 binary variables and were heavily reduced by presolve to two constraints with 626,907–632,612 binary variables, effectively forming large knapsack-type problems. By contrast, the extinction risk single-objective formulation (Eq. (3)) and the GP formulations (Eqs. (A.26)–(A.33)) incorporated additional continuous variables and general constraints resulting from the PWL approximation of the species–area relationship (Eqs. (A.9)–(A.12), with constraints (A.14)–(A.16)) and the deviation variables. Prior to presolve, these formulations included ~463–471 continuous variables and 154 general constraints. After presolve, models contained ~4,700–4,900 continuous variables, ~590,000–633,000 binary variables, and 153 SOS constraints, reflecting the linearized species-level structure (Table B1).

**Runtime and solution quality.** All models were solved at the root node (one explored node). Solver-reported wall-clock times ranged from a few seconds for the simplest single-objective formulations to approximately one minute for the GP models, with final optimality gaps below 0.001% (e.g., 0.0009% for extinction-risk optimization and 0.0006% for the feasibility-excluded GP model). End-to-end pipeline runtimes—including data preprocessing, model construction, optimization, and post-processing—ranged from ~20–650 s for Step-1 runs and ~640–730 s for Step-2 runs, with total workflow times of ~1,350 s (feasibility-included) and ~1,530 s (feasibility-excluded) (Table B1).

**Table B1. Computational characteristics of the optimization runs.**

The table reports model size (number of constraints [Rows], total variables [Cols]—including binary and continuous variables—, and nonzero coefficients), presolve reductions, solver time, final optimality gap, and end-to-end pipeline runtime. Solver time corresponds to the wall-clock time reported by Gurobi logs.

| Run | Formulation | Rows | Cols | Nonzeros | Bin vars | Cont vars | Presolved rows | Presolved cols | Solver time (s) | Final gap | Pipeline time (s)* |
|---|---|---|---|---|---|---|---|---|---|---|---|
| $SO_E$ | Single-objective (Extinction Risk) | 180,762 | 813,373 | 12,225,958 | 812,910 | 463 | 614 | 594,628 | 7.41 | 0.0009% | 582.29 |
| $SO_c$ | Single-objective (Carbon Storage) | 180,300 | 812,910 | 1,419,662 | 812,910 | 0 | 2 | 626,907 | 11.19 | 0.0000% | 20.27 |
| $SO_w$ | Single-objective (Water Provision) | 180,300 | 812,910 | 1,419,662 | 812,910 | 0 | 2 | 632,612 | 2.33 | 0.0000% | 36.70 |
| $SO_f$ | Single-objective (Restoration Feasibility) | 180,300 | 812,910 | 1,419,662 | 812,910 | 0 | 2 | 632,612 | 32.09 | 0.0000% | 41.59 |
| $MO_{F\text{-}ex}$ | Multi-objective (Feasibility-excluded) | 180,766 | 813,381 | 13,831,088 | 812,910 | 471 | 772 | 637,515 | 65.03 | 0.0006% | 734.03 |
| $MO_{F\text{-}in}$ | Multi-objective (Feasibility-included) | 180,767 | 813,381 | 14,644,000 | 812,910 | 471 | 772 | 637,517 | 53.02 | 0.0000% | 643.34 |

*Pipeline time includes model construction, optimization, and post-processing steps.

## Appendix C. Complementary results and spatial diagnostics

**Table C1. Latitudinal statistics of single-objective and multi-objective solutions.**

Latitudinal statistics were computed by aggregating selected planning units into 1-km latitudinal bands based on their centroid latitude. For each objective and balanced solution, the table reports the number of latitudinal bands containing at least one selected unit (# Bands), the mean and standard deviation of the number of selected units per band (Mean ± SD), the minimum and maximum number of units per band (Min–Max), the coefficient of variation (CV), and the interquartile range (IQR, 25th–75th percentile). Together, these indicators describe whether a given optimization results in spatially concentrated patterns (few bands with high counts per band) or in distributions that are more evenly dispersed along latitude (many bands with lower and less variable counts). Because all solutions select the same total number of units, these differences directly reflect contrasting spatial distributions along the north–south gradient. Higher CV and IQR values correspond to greater latitudinal heterogeneity, whereas lower values correspond to relatively homogeneous distributions.

| Objective | # Bands | Mean ± SD | Min–Max | CV | IQR (25–75%) |
|---|---|---|---|---|---|
| Extinction Risk Reduction | 4,253 | 57.3 ± 35.6 | 1–160 | 0.622 | 30–80 |
| Carbon Storage | 2,629 | 92.8 ± 54.0 | 1–253 | 0.582 | 57–130 |
| Water Provision | 3,573 | 68.3 ± 55.7 | 1–225 | 0.816 | 22–105 |
| Restoration Feasibility | 2,774 | 87.9 ± 57.4 | 1–251 | 0.653 | 47–118 |
| Balance among Objectives (*Feasibility-excluded* scenario) | 3,820 | 63.8 ± 46.9 | 1–189 | 0.735 | 24–98 |
| Balance among Objectives (*Feasibility-included* scenario) | 4,150 | 58.8 ± 41.7 | 1–208 | 0.71 | 25–86 |

**Table C2. Objective-level performance across single-objective and multi-objective solutions.**

The table reports normalized performance scores (0–100) for each objective (rows) evaluated under single-objective and multi-objective optimization solutions (columns). Single-objective solutions correspond to extinction risk reduction (ER), carbon storage (CS), water provision (WP), and restoration feasibility (RF). Multi-objective solutions represent the Balance of Objectives (BO) for the feasibility-excluded (BO F-ex) and feasibility-included (BO F-in) scenarios. Scores are normalized within each objective, using the corresponding single-objective optimum as the reference baseline (value = 100.0; bold). The **Cross-solution performance** column summarizes, for each objective, its average performance across the remaining single-objective optimizations (computed as the mean of the off-diagonal values in that row). Conversely, the **Cross-objective performance** row reports, for each solution, the average normalized performance achieved across the non-targeted objectives (computed as the mean of the off-diagonal values in that column, and extended to the multi-objective solutions). Values shown in green correspond to relatively high performance, whereas values shown in red indicate comparatively low performance, highlighting asymmetric trade-offs among criteria. Note that the Cross-solution performance column provides a comparative diagnostic of objective compatibility and does not correspond to an actual spatial optimization run.

| | **Single-objective optimization** | | | | | **Multi-objective optimization** | |
|---|---|---|---|---|---|---|---|
| **Objective** | **ER** | **CS** | **WP** | **RF** | **Cross-solution performance** | **BO (F-ex)** | **BO (F-in)** |
| Extinction Risk Reduction | **100.0** | **51.3** | **66.0** | **47.6** | 55.0 | 84.6 | 85.8 |
| Carbon Storage | **45.4** | **100.0** | **71.0** | **30.6** | **49.0** | 86.1 | 82.0 |
| Water Provision | 87.9 | **90.4** | **100.0** | **79.4** | **85.9** | 97.2 | 94.8 |
| Restoration Feasibility | **72.4** | 65.0 | **51.0** | **100.0** | 62.8 | 62.1 | 73.2 |
| **Cross-objective performance** | 68.5 | **68.9** | 62.7 | **52.6** | 63.2 | 82.5 | 83.9 |

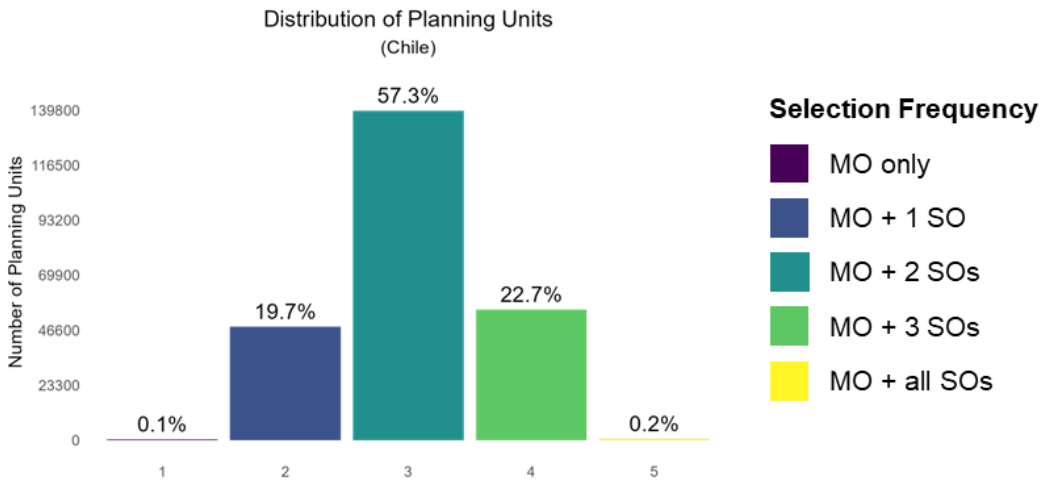


**Fig. C1 | National distribution of selection frequency of planning units across the optimization framework.** Bar plot shows the number and proportion of planning units at national scale, grouped by their selection frequency across all optimization runs. Selection frequency indicates how consistently a unit is prioritized within the framework, combining its selection in the compromise multi-objective (MO) solution (Step 2) with its selection in the single-objective (SO) optimizations (Step 1). Values on the x-axis range from 1 to 5: a value of 1 corresponds to units selected exclusively in the multi-objective solution (MO only), while values 2 through 5 correspond to units also selected in one to four single-objective solutions (MO + 1–4 SOs). This figure provides a national-scale summary of the regional selection-frequency patterns detailed in Fig. 5.

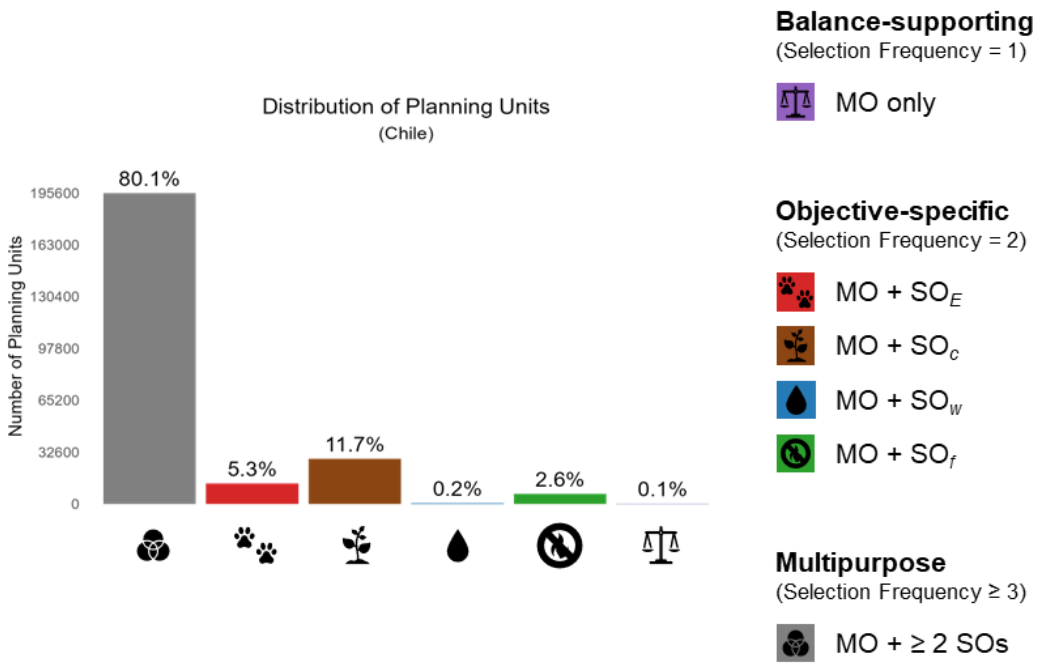


**Fig. C2 | National distribution of the functional roles of planning units in the multi-objective solution.** The bar plot shows the absolute number and proportional distribution of planning units assigned to each functional role at the national scale in Chile, based on their selection frequency ($\rho_i$) across the multi-objective (MO) solution and the four single-objective (SO) optimizations. Multipurpose units correspond to those selected in the MO solution and in two or more SO runs (selection frequency ≥ 3; MO + ≥ 2 SOs). Objective-specific units are selected in the MO solution and exactly one SO run (selection frequency = 2; MO + 1 SO), and are further classified by their specific target: extinction risk reduction ($SO_E$), carbon storage ($SO_c$), water provision ($SO_w$), or restoration feasibility ($SO_f$). Balance-supporting units correspond to units selected exclusively in the MO solution (selection frequency = 1; MO only). Percentages indicate the relative contribution of each functional role to the total number of units selected in the multi-objective solution across continental Chile. This figure provides a national-scale summary of the functional role patterns shown spatially in Fig. 6.